Highlights of poster session 2 (Rosé)

(a rather inhomogeneous session!)

Les Mûriers, Chinon rosé 2013

Christian Joram, CERN PH

23 posters, but I received only material from 12 authors (in yellow).

Abstract ID	Board ID	Primary Author	Title
34392	2	Liu Zheng	Quality control of the MPPC TSV arrays, and Modules (MPPC with crystal) for the External Plate of EndoTOF-PET US detector
34435	5	Vandenbussche Vincent	Dual ended readout by SiPMs on LYSO crystal bars: energy and spatial response
34653	8	Veloso Joao	easyPET: a user friendly PET system for didactic purposes
34696	11	Preziosi Enrico	A novel method for gamma-rays depth of interaction determination on monolithic scintillation crystals
34185	14	Kanno Ikuo	Effective Atomic Number Measurement with Energy-resolved X-ray Computed Tomography
34546	17	Spadola Sara	Development and Performance Characterization of Intraoperative Positron Probes for Tumor Surgery
34587	20	Castro Ismael	DRIM-PET: Dual-ended Readout Innovative Method for Positron Emission Tomography
34613	23	Moutinho Luis	Brachytherapy dosimeter with silicon photomultipliers
33901	26	Vladimir Morozov	Afterpulses of the H6780 and R7600U?200 Metal Channel Photomultiplier Tubes
34482	29	Heng Yuekun	The Central Detector of JUNO
34548	32	Yoshitaka Hanabata	Evaluation of the basic properties of the newly developed 1.5' size PMTs R-11920-100 and R-12992-100 from Hamamatsu Photonics and D569/2SA from Electron Tubes Enterprises
34929	38	Kapusta Maciej	ADIT 1' photomultiplier with anode's screening grid ? timing studies.
35306	41	Hugon Christophe	Step by step GEANT4 simulation for PhotoTubes
35746	44	Lubsandorzhiev Bayarto	Studies of vacuum photomultipliers at extremely low thresholds, photoelectron backscattering and photon detection efficiency
37494	47	Fink David	PMT Module Characterization Test Bench for the MAGIC IACT Telescopes
34585	50	Croci Gabriele	Light Response of LaBr3 and YAP Scintillators to 5-20 MeV protons for applications to thin-foil proton recoil neutron spectrometer
34612	53	Cinti Maria Nerina	Excellent pulse height uniformity response of a new LaBr3(Ce) scintillation crystal for gamma ray imaging
34718	56	Shunsuke Kurosawa	Perfomance of Ce:La-GPS scintillator with an MPPC
34722	59	Ponomarenko Sergey	Nanostructured organosilicon luminophores for highly efficient plastic scintillators and spectral shifters
35428	62	Liu Ben	FLUKA-based simulation for LYSO gamma detectors in proton therapy
35760	65	Kamada Kei	Development of a proto-type detector using novel Ce:GAGG scintillator arrays for high resolution radiation imaging
33307	68	Minot Michael	Pilot Production & Commercialization of LAPPD?
34738	74	Tremsin Anton	Optimization of High Count Rate Photon Counting Detector with Microchannel Plates and Quad Timepix readout

THE PICOSEC
MC-NET PROJECT

ENDO TOFPET US
Endoscopic TOFPET & Ultrasound

MARIE CURIE ACTIONS

Quality control of the MPPC TSV arrays, and Modules (MPPC with crystal) for the External Plate of EndoTOF-PET US detector.

Zheng Liu etal.

SEVENTH FRAMEWORK PROGRAMME

PicoSEC MC-Net Project is supported by a Marie Curie Early Initial Training Network Fellowship of the European Community's Seventh Framework Programme under contract number (PITN-GA-2011-289355-PicoSEC-MCNet). EndoTOFPETUS has received funding from the European Union 7th Framework Program (FP7/ 2007-2013) under Grant Agreement No. 256984.

CERN DESY UNIVERSITÀ DEGLI STUDI DI MILANO BICOCCA

Overview

- The aim of the EndoTOFPET-US collaboration is to develop an imaging tool combining Ultrasound with Time-Of-Flight PET into an endoscopic imaging device.
- The objective of the TOF-PET scanner is to reach a CTR of 200 ps FWHM.
- The external PET detector is 256 matrices of 4 × 4 LYSO crystals with size of 3.5 × 3.5 × 15mm^3, coupled to 256 Hamamatsu TSV-MPPC arrays (S12643-050CN).
- A full characterization of the MPPC arrays has been performed;
  - Voltage equivalent to the zero gain,
  - Current versus applied bias voltage,
  - Dark count rate (DCR) at level of 0.5 p.e.,
  - Single Photon Time Resolution (SPTR),
  - The CTR of each module (crystal glued on MPPC array),

Measurement result

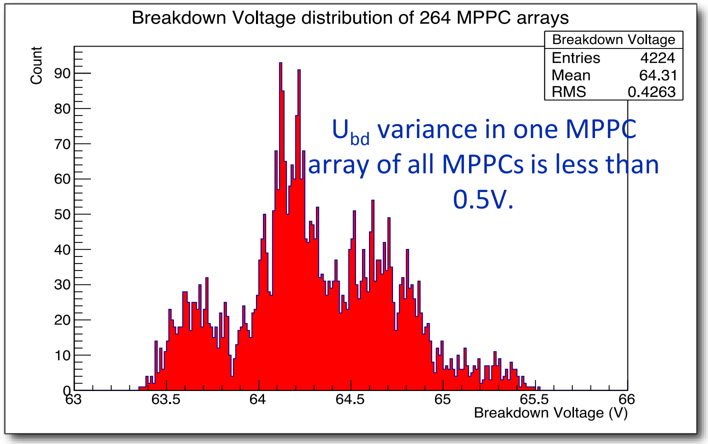

Distribution of breakdown

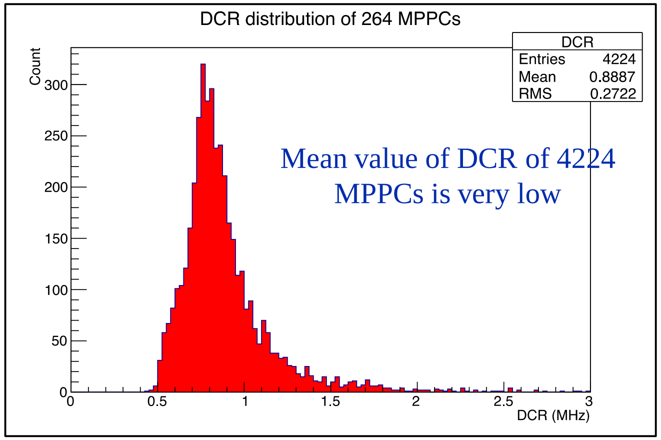

Distribution of DCR.

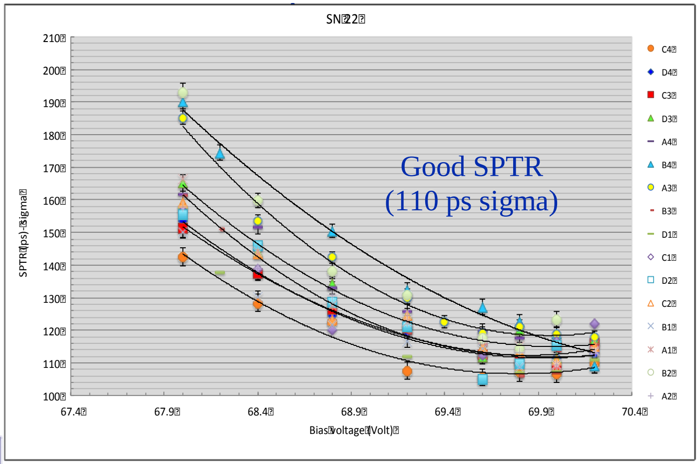

SPTR as a function of bias voltage

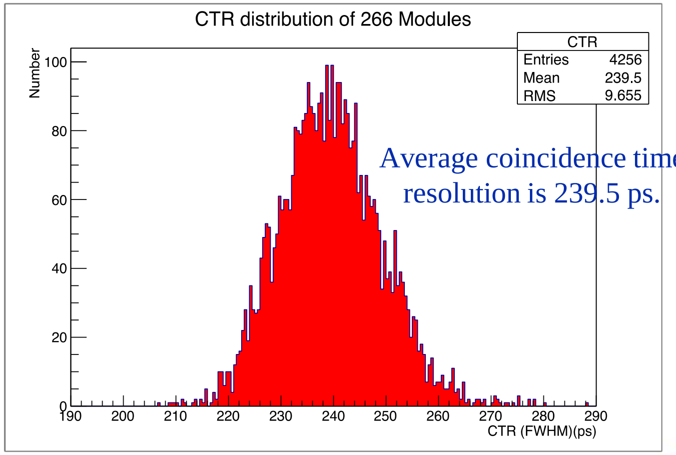

For such a large number of readout units (crystals + MPPC array), such performance is very promising!

Skipped !

- ID 5
- Vandenbussche Vincent
- Dual ended readout by SiPMs on LYSO crystal bars: energy and spatial response

Comparison of simulated data with a analytical model

NDIP2014

A novel method for gamma-rays depth of interaction determination on monolithic scintillation crystals

SAPIENZA
UNIVERSITÀ DI ROMA

R. Pani[1], P. Pani[2], E. Preziosi[3], S. Lo Meo[4], M.N. Cinti[1], R. Pellegrini[1], A. Fabbri[5], M. Bettiol[6], M. Longo[6] and R. Scafé[1]

[1] Department of Molecular Medicine, Sapienza University of Rome, Rome, Italy
[2] Nikhef, Amsterdam, The Netherlands
[3] Morphofunctional Science – Biophysics, Doctorate School of Biology and Molecular Medicine, Sapienza University of Rome, Rome, Italy
[4] ENEA, Bologna, Italy
[5] Department of Physics, Roma Tre University, Rome, Italy
[6] Medical Physics Post Graduate School, Sapienza University of Rome, Rome, Italy

Depth of Interaction (*DoI*)

Normal incidence

Angled incidence

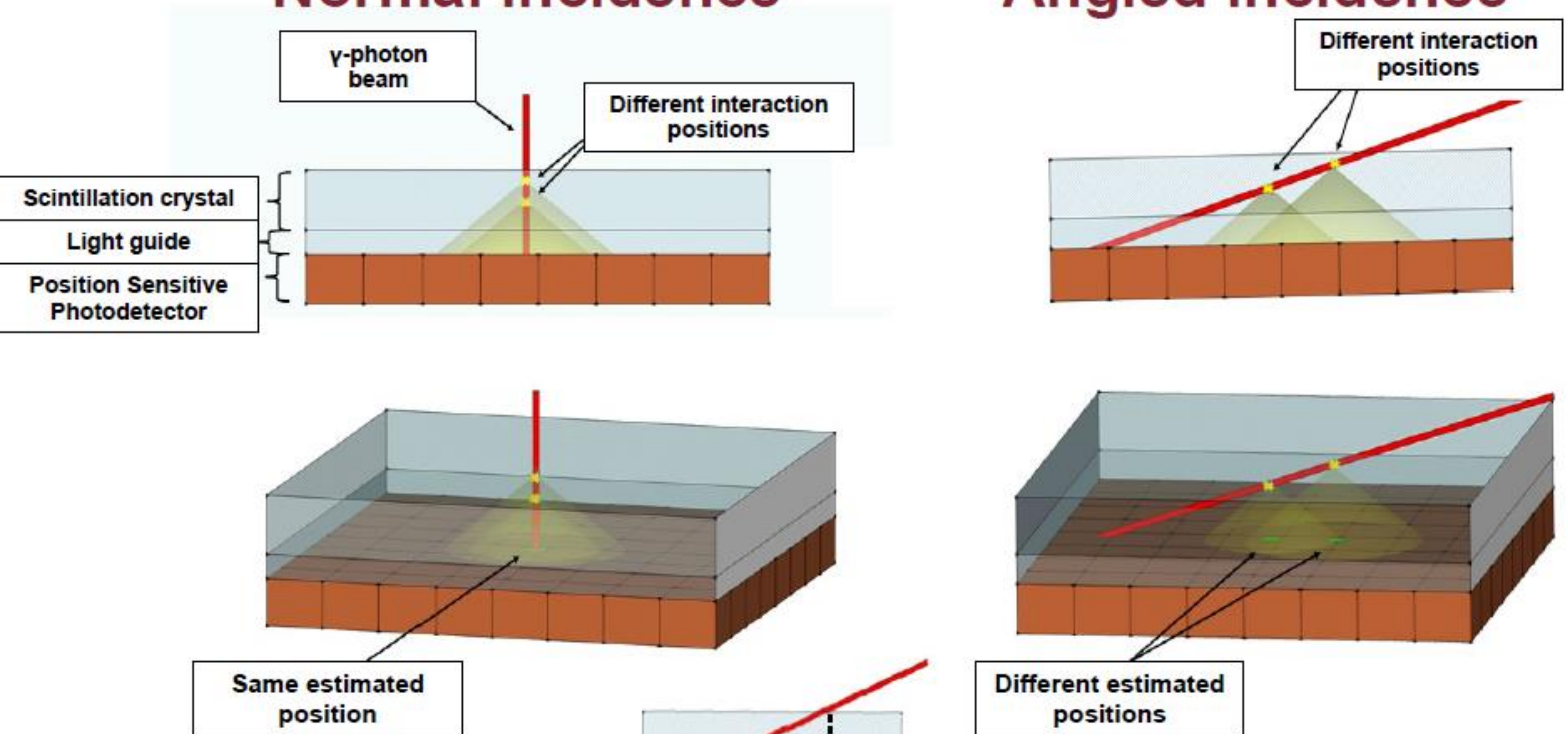

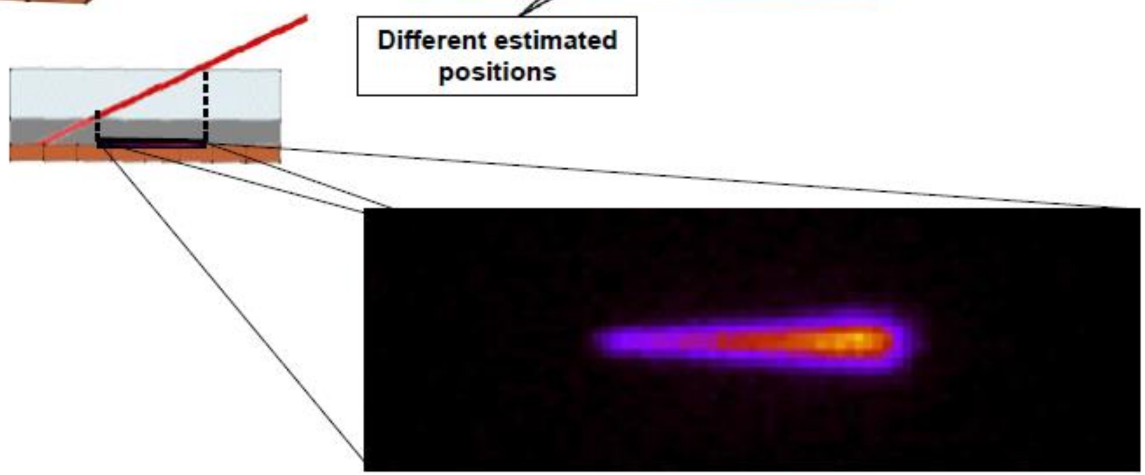

As a consequence of the depth of interaction effect, the image of a tilted collimated beam is blurred along one direction.

The *N/I* parameter

Scrimger and Baker function

This function, obtained in 1967, describes the scintillation light distribution on the photodetection plane.

$$I_r = \frac{I_0}{[1+(r/t)^2]^{3/2}}$$

t
is the depth of interaction

t is measured from detection plane

Integrating the function on the photodetection plane:

$$N = \int dx \int dy \frac{I}{\left[1 + \frac{x^2+y^2}{t^2}\right]^{3/2}}$$

$\Longrightarrow$ In polar coordinates $\Longrightarrow$

$$N = \int d\theta \int dr \frac{I \cdot r}{\left[1 + \frac{r^2}{t^2}\right]^{3/2}} = 2\pi \int dr \frac{I \cdot r}{\left[1 + \frac{r^2}{t^2}\right]^{3/2}}$$

$$N = 2\pi \left[- \frac{I \cdot t^2}{\sqrt{1 + \frac{r^2}{t^2}}} \right]_0^{+\infty} = 2\pi \cdot I \cdot t^2 \Longrightarrow \boxed{N/I = 2\pi \cdot t^2}$$

The smaller t, the more peaky is the distribution

$$\frac{N}{I} \propto t^2 \equiv DoI^2$$

N is the value of the integral of the light (charge) distribution

I is the value of the maximum of the light (charge) distribution

N/I depth selection

The Figure shows the comparison between the theoretical trend and the behaviour obtained from events coming from different depth of interaction in the simulated data. The points represent the layer mean value of the N/I value of the events coming from each 0,5mm-thick layer, and the bars the standard deviation of the layer distributions.

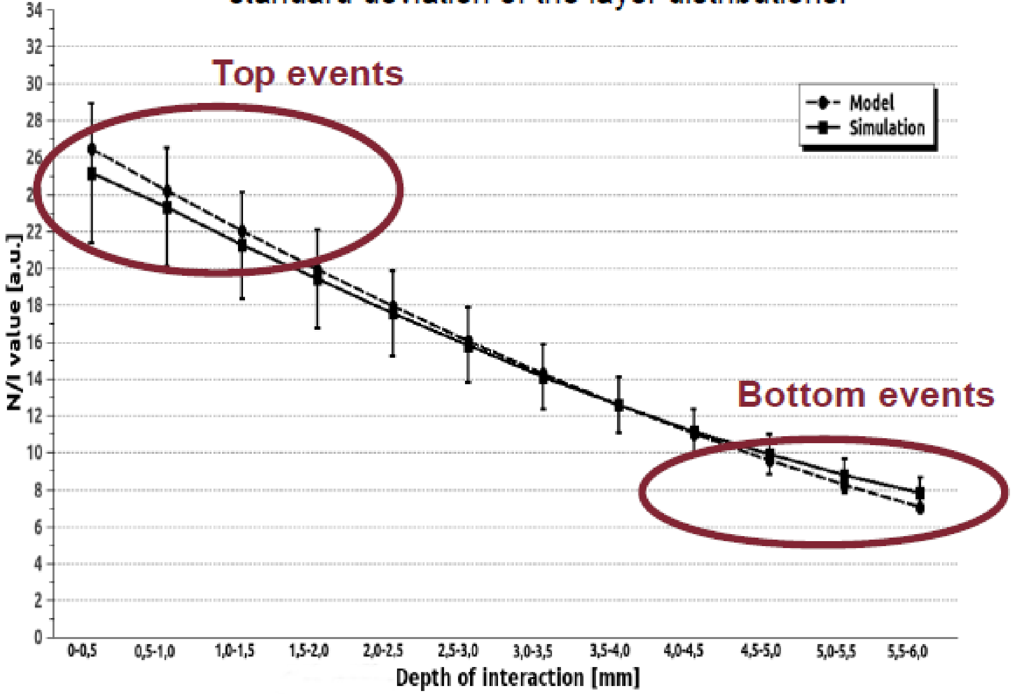

As showed, the parameter follows the behaviour expected from the theoretical model, and it allows to select the events as a function of their depth of interaction.

Results

By choosing specific windows of the *N/I* parameter, it is possible to obtain different images as a function of the depth of interaction

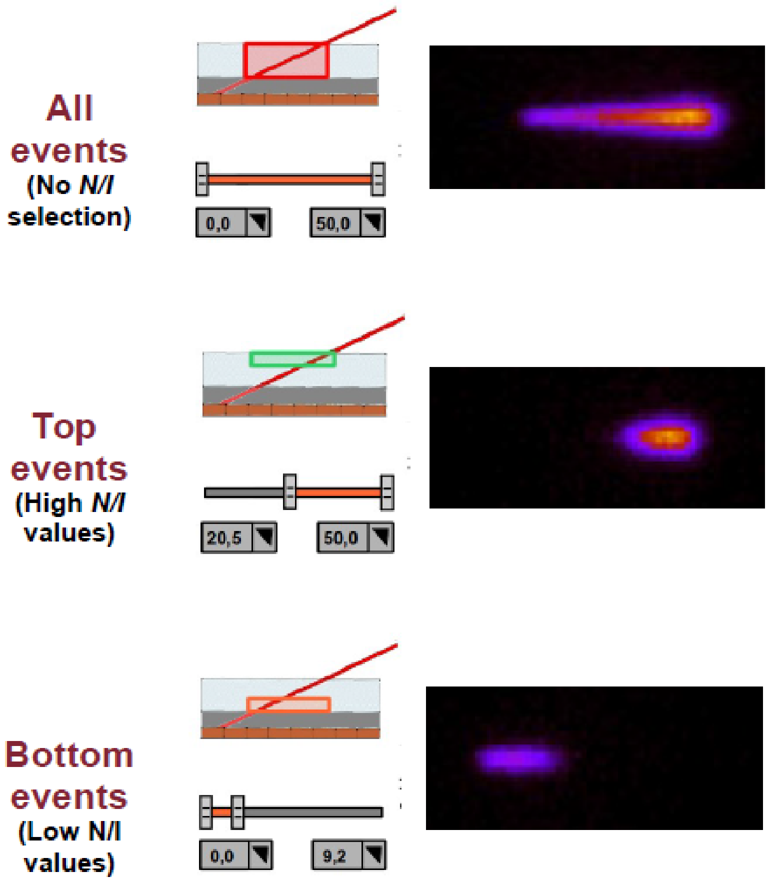

Effective Atomic Number Measurement with Energy-resolved X-ray Computed Tomograhy

I. Kanno, Y. Yamashita, M. Kimura, F. Inoue
Department of Nuclear Engineering,
Kyoto University, Japan

Effective Atomic Number

- tissue segmentation in computed tomography (CT)
- ion range in a human body

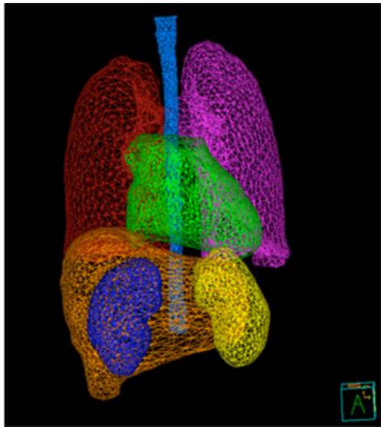

- Can be measured with using two monochromatic X-rays,

but not in hospitals

Energy-resolved X-ray CT

- Current mode detector system,

  transXend detector

  Current measurement of X-rays

  Unfolding

  Energy distribution

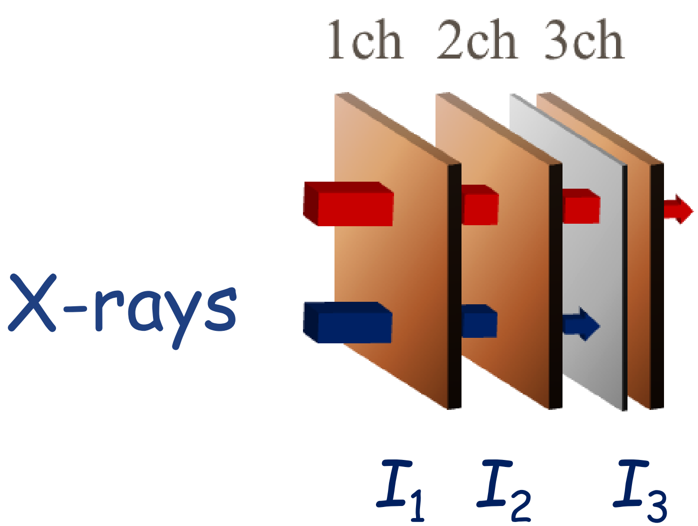

$$\begin{pmatrix} I_1 \\ I_2 \\ I_3 \end{pmatrix} = \begin{pmatrix} R_{11} & R_{12} & R_{13} \\ R_{21} & & \\ R_{31} & & R_{33} \end{pmatrix} \begin{pmatrix} Y_1 \\ Y_2 \\ Y_3 \end{pmatrix}$$

Response function

Energy distribution

Effective Atomic Number Measurements

$$\frac{\mu(E_1)}{\mu(E_2)} = f(Z)$$

- $\mu(E)$: linear attenuation coefficient at energy E

- Energy-resolved CT ➡ $\mu(E_1)$, $\mu(E_2)$ with one exposure

- Z_{eff} Al 13.1 (0.8%)
  Acrylic 6.46 (0.2%)

⬇

Applied to diluted sugar solution (soft tissue)

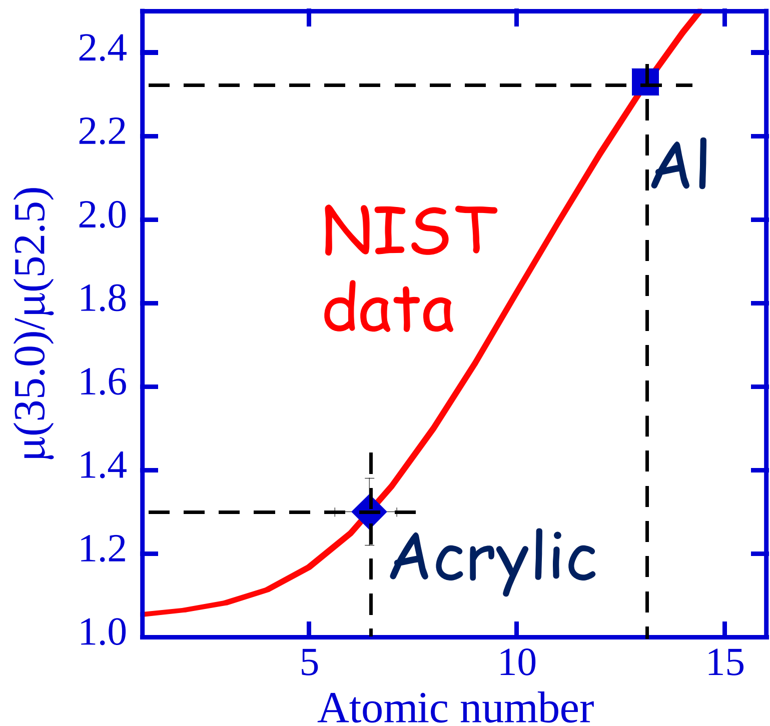

Skipped !

- ID 17
- Spadola Sara
- Development and Performance Characterization of Intraoperative Positron Probes for Tumor Surgery

ID-20, Wednesday
Ismael Castro

University of Aveiro, Portugal
Department of Physics & i3n
DRIM group

DRIM-PET

Dual-ended **R**eadout **I**nnovative **M**ethod for **PET**

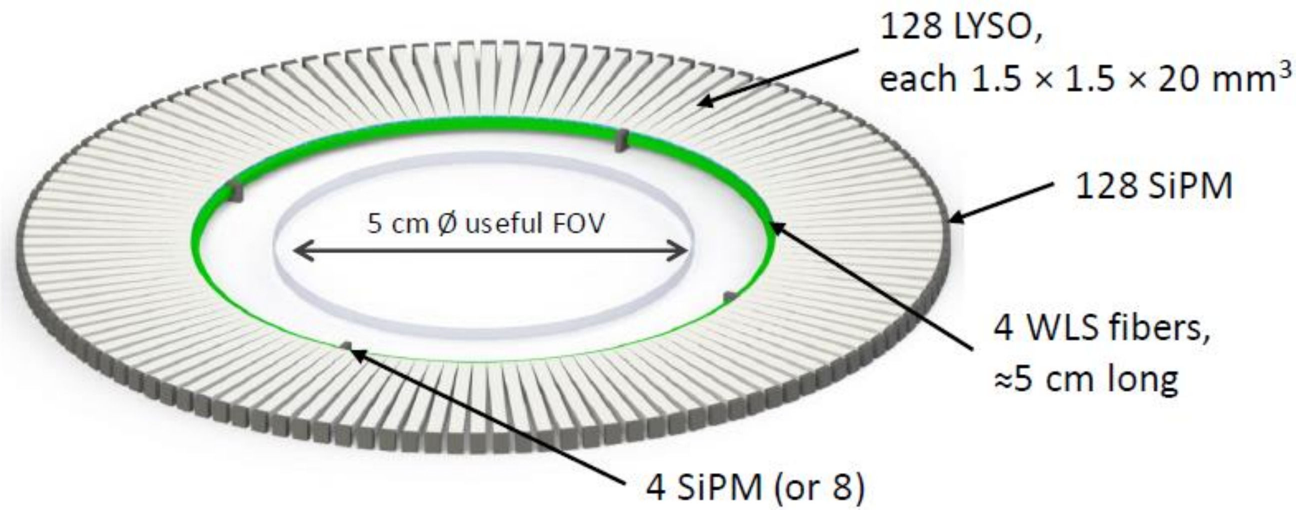

- Light levels collected by each SiPM simulated with GATE, for different configurations

⇩

Best performance obtained for dual-ended SiPM readout of WSF:

DOI resolution ≈ 1-2 mm FWHM

- Measurement of DOI demonstrated experimentally.

A simple and low-cost method to measure depth of interaction (DOI):

- outer end of each LYSO crystal coupled directly to SiPM
- inner end of each group of 32 crystals coupled to a wavelength-shifting fiber, read out by 1 or 2 SiPM → **≈ half # of channels, simpler electronic readout**

ID-20, Wednesday
Ismael Castro

University of Aveiro, Portugal
Department of Physics & i3n
DRIM group

DRIM-PET: Dual-ended **R**eadout **I**nnovative **M**ethod for **PET**

1) GATE simulation of the amount of light collected by each SiPM (1 cell):

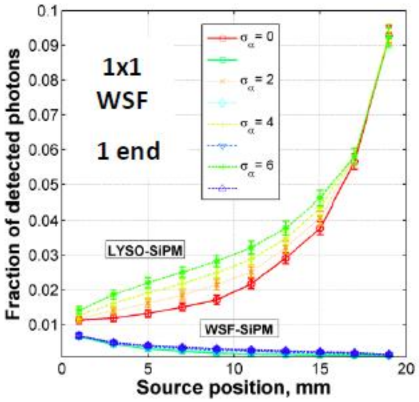

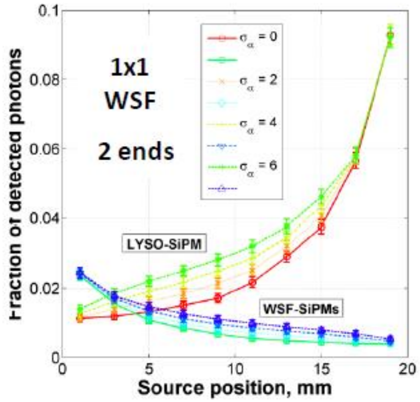

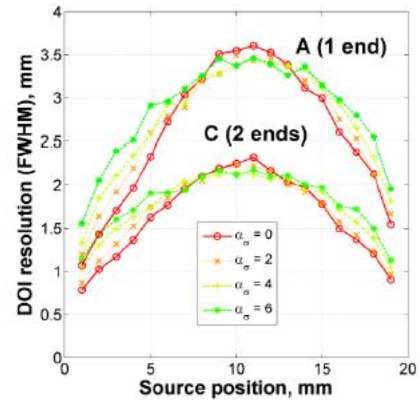

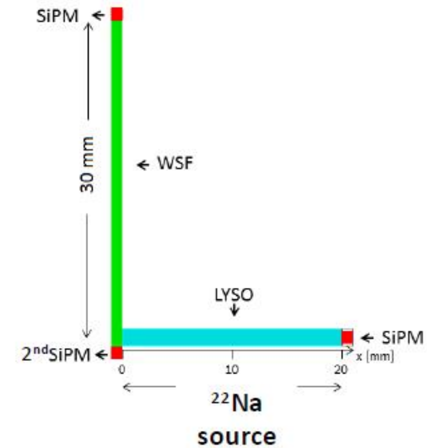

2) Experimental demonstration:

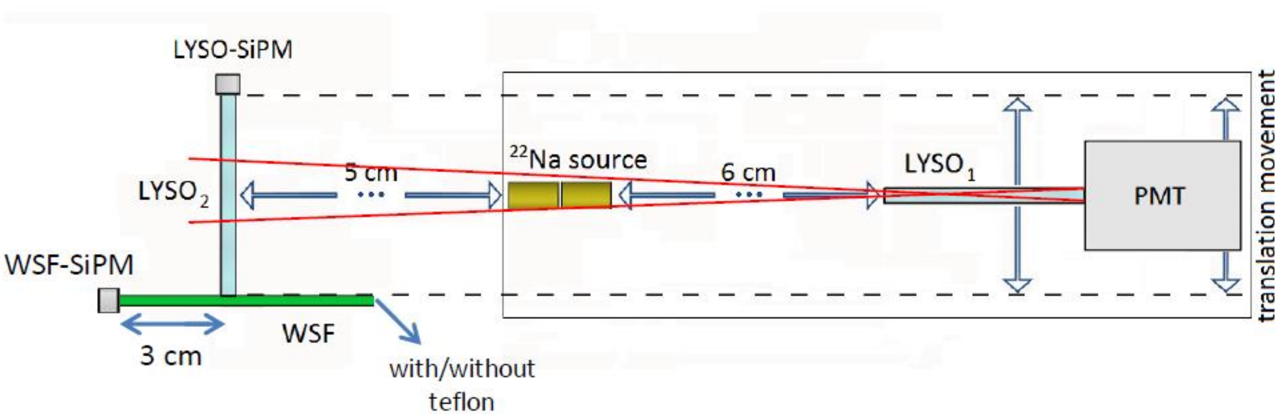

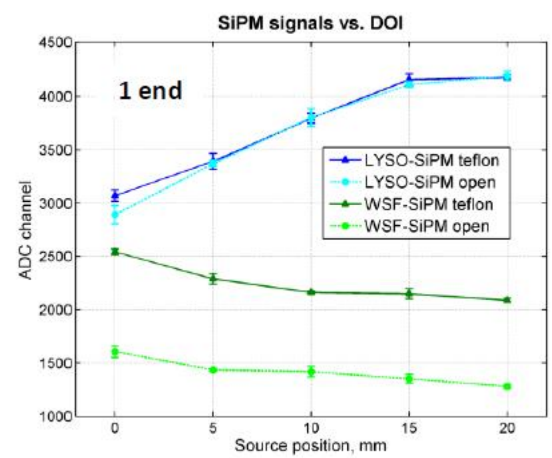

ID-20, Wednesday
Ismael Castro

University of Aveiro, Portugal
Department of Physics & i3n
DRIM group

DRIM-PET: Dual-ended Readout Innovative Method for PET

1) GATE simulation of the amount of light collected by each SiPM (1 cell):

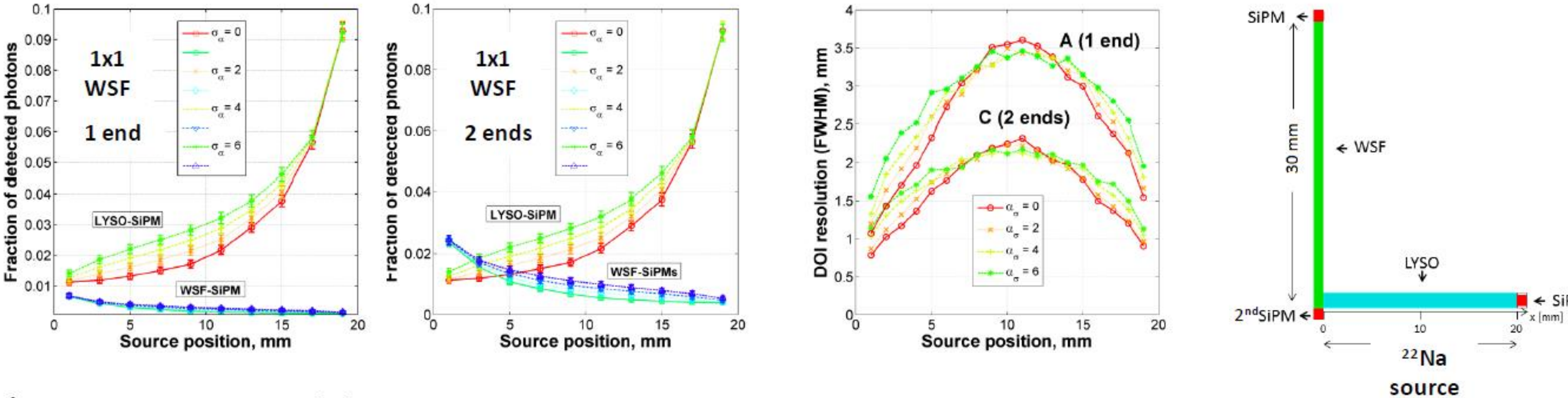

2) Experimental demonstration:

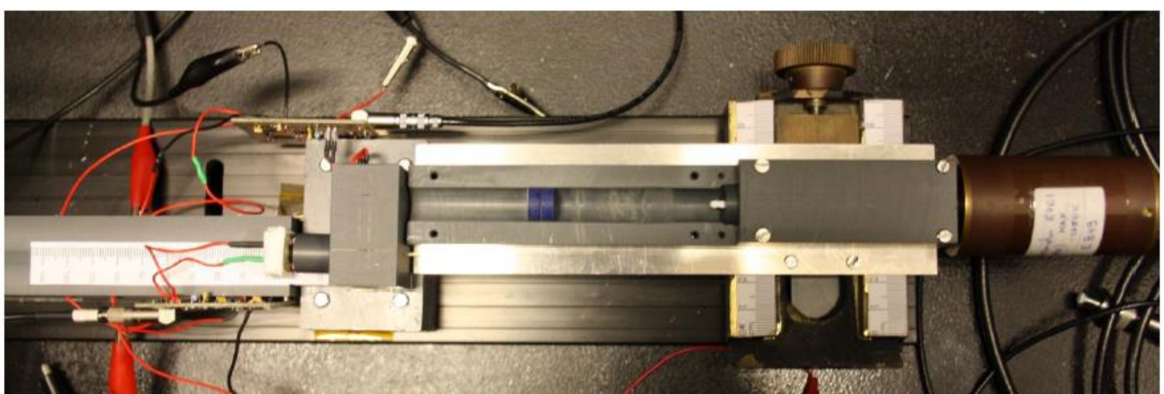

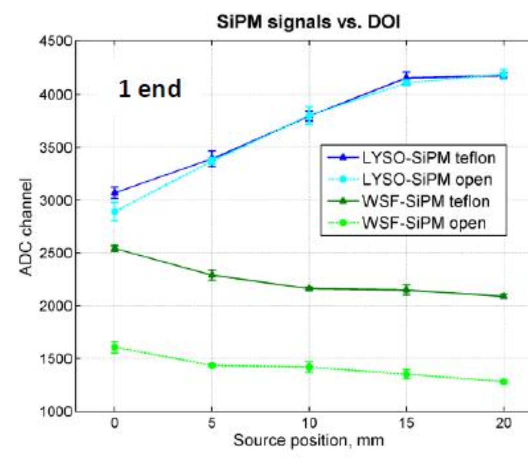

ID 23

Brachytherapy dosimeter with silicon photomultipliers

LM Moutinho *et al.* I3N, Physics Department, University of Aveiro, Portugal

A high sensitive dosimeter was developed. The dosimeter comprises a sensitive probe with a scintillating optical fiber. SiPMs are used to read the scintillation light. This configuration allows in-vivo applications such as brachytherapy.

Dose calibration - setup

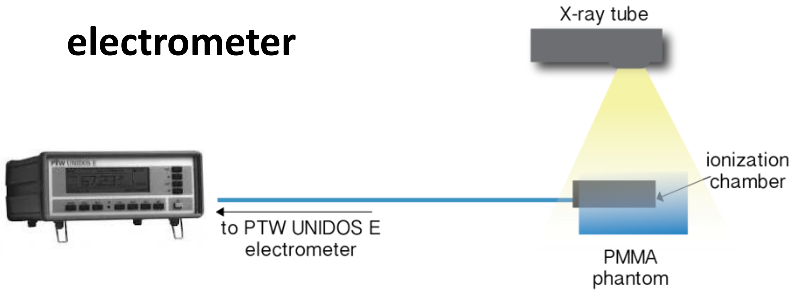

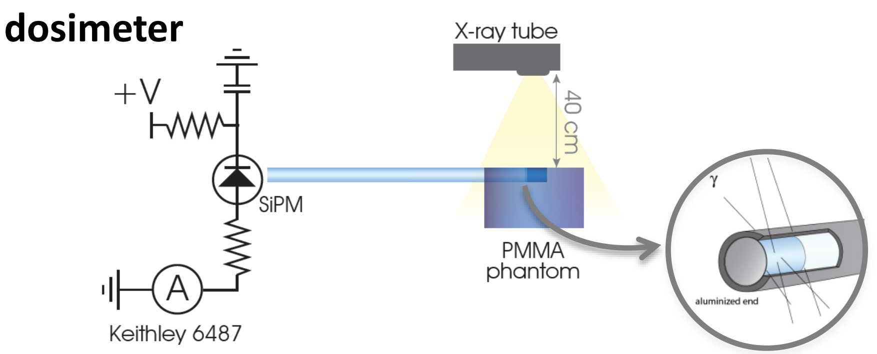

calibration results

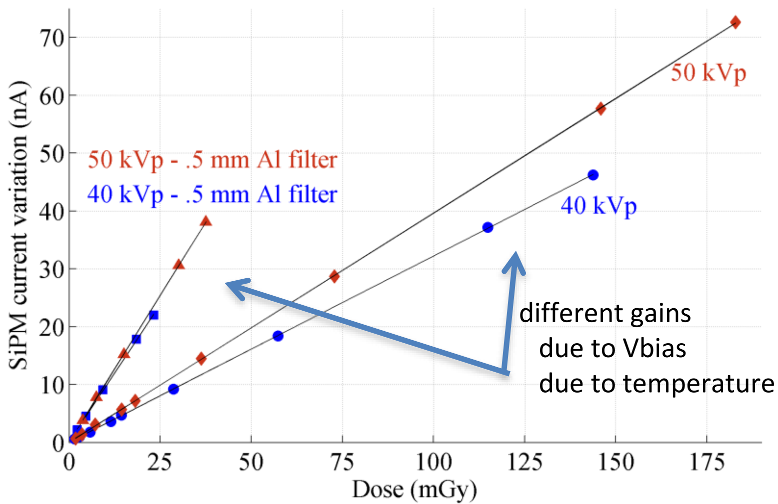

- capable to measure small dose variations low as 700µGy
- dosimeter response is linear with the dose increase
- for the same dose at different energies the response is not the same
    - this is due to temperature variation during the calibration
    - possible non linearity of the plastic scintillator at low energies

Afterpulses of the H6780 and R7600U-200 Metal Channel Photomultiplier Tubes

Morozov V.A., Morozova N.V.
Joint Institute for Nuclear Research, Dubna, Russia

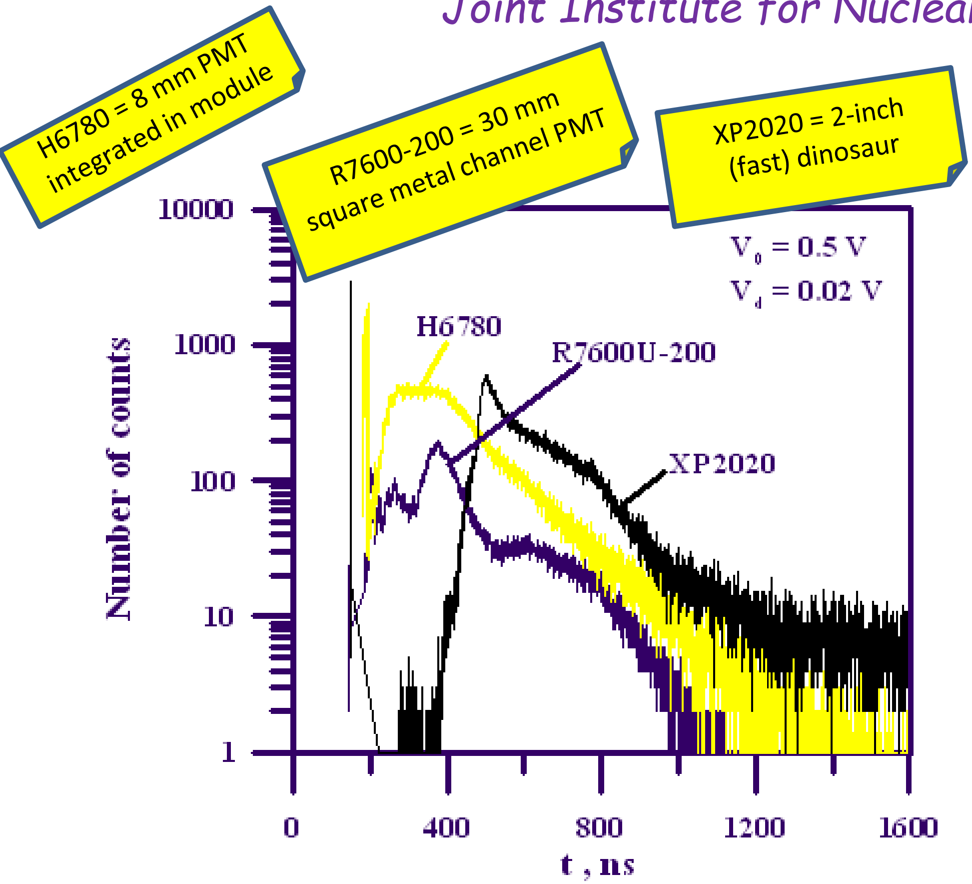

Fig.1. Time distributions of afterpulses in photomultipliers of various types.

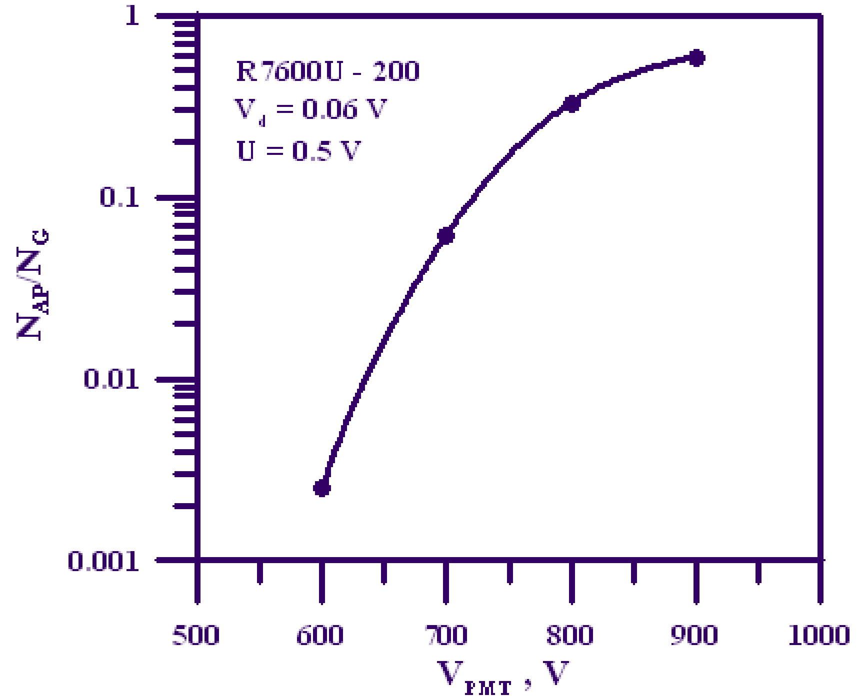

Fig.2. Dependence of the afterpulse intensity on the R7600U-200 PMT voltage.

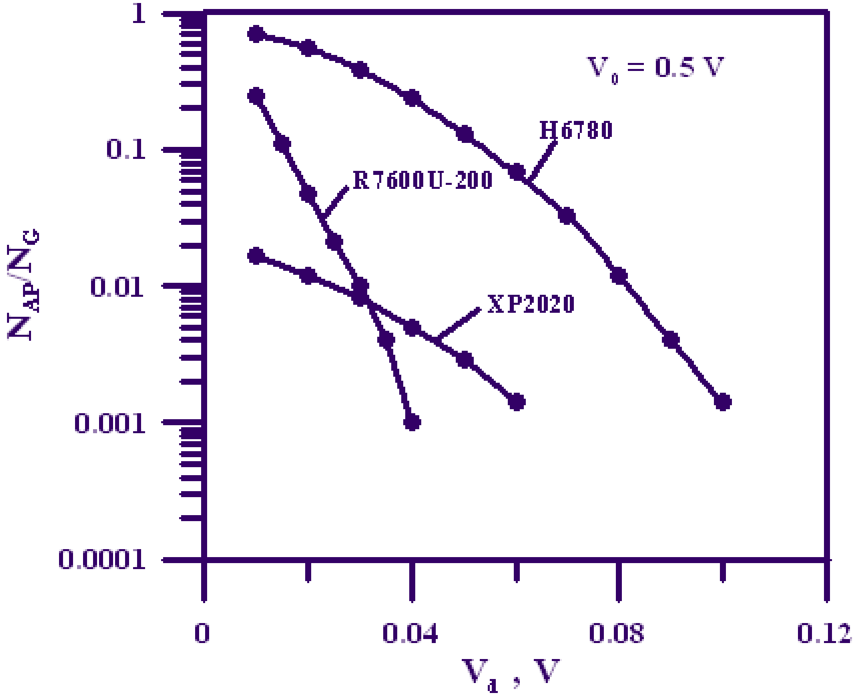

Fig.3.Comparative characteristics of the afterpulse intensities for the H6780, R7600U-200 and XP2020.

*

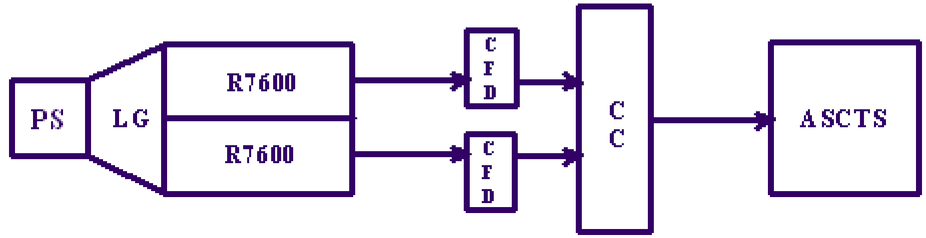

Fig.4.Block diagram of the delayed-coincidence spectrometer with a double photodetector.

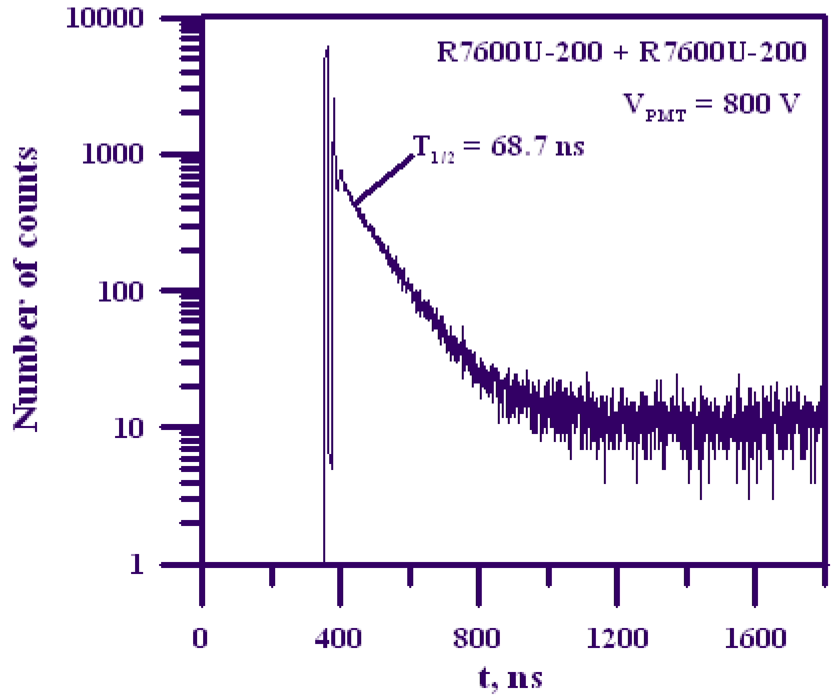

Fig.4*. Half-life measurements for the 59-keV state in ^{237}Np using the double photodetector with the R7600U-200.

Skipped !

- ID 29
- Heng Yuekun
- The Central Detector of JUNO

- ID 32
- Yoshitaka Hanabata
- Evaluation of the basic properties of the newly developed 1.5' size PMTs R-11920-100 and R-12992-100 from Hamamatsu Photonics and D569/2SA from Electron Tubes Enterprises

- ID 38
- Kapusta Maciej
- ADIT 1' photomultiplier with anode's screening grid ? timing studies.

- ID 41
- Hugon Christophe
- Step by step GEANT4 simulation for PhotoTubes

- ID 44
- Lubsandorzhiev Bayarto
- Studies of vacuum photomultipliers at extremely low thresholds, photoelectron backscattering and photon detection efficiency

MAGIC Camera Module Measurement – Setup Block Diagram

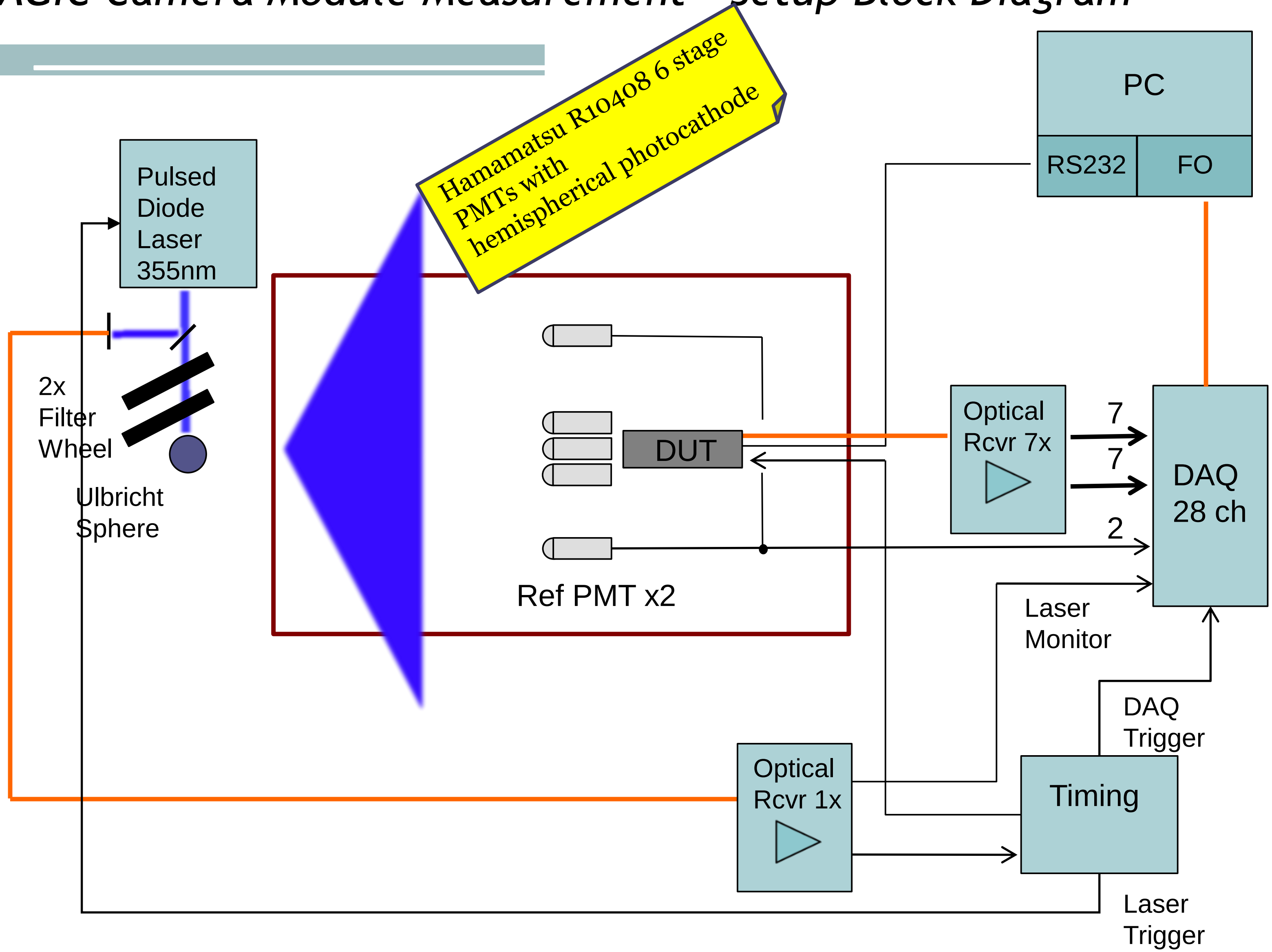

MAGIC Camera Module Measurement – Setup DAQ / Rcvr / Timing / Power

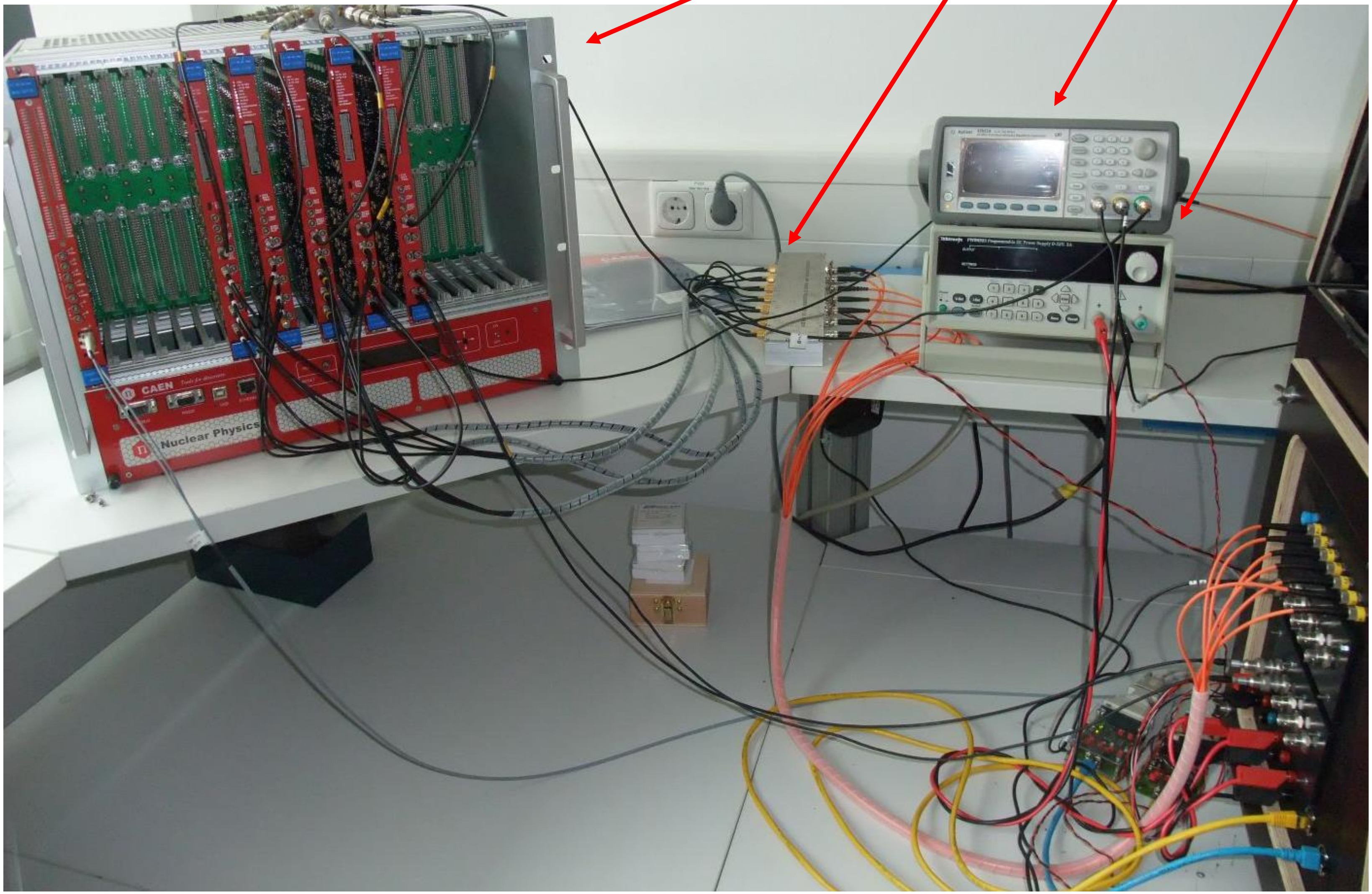

MAGIC Camera Module Measurement – Setup Enclosure

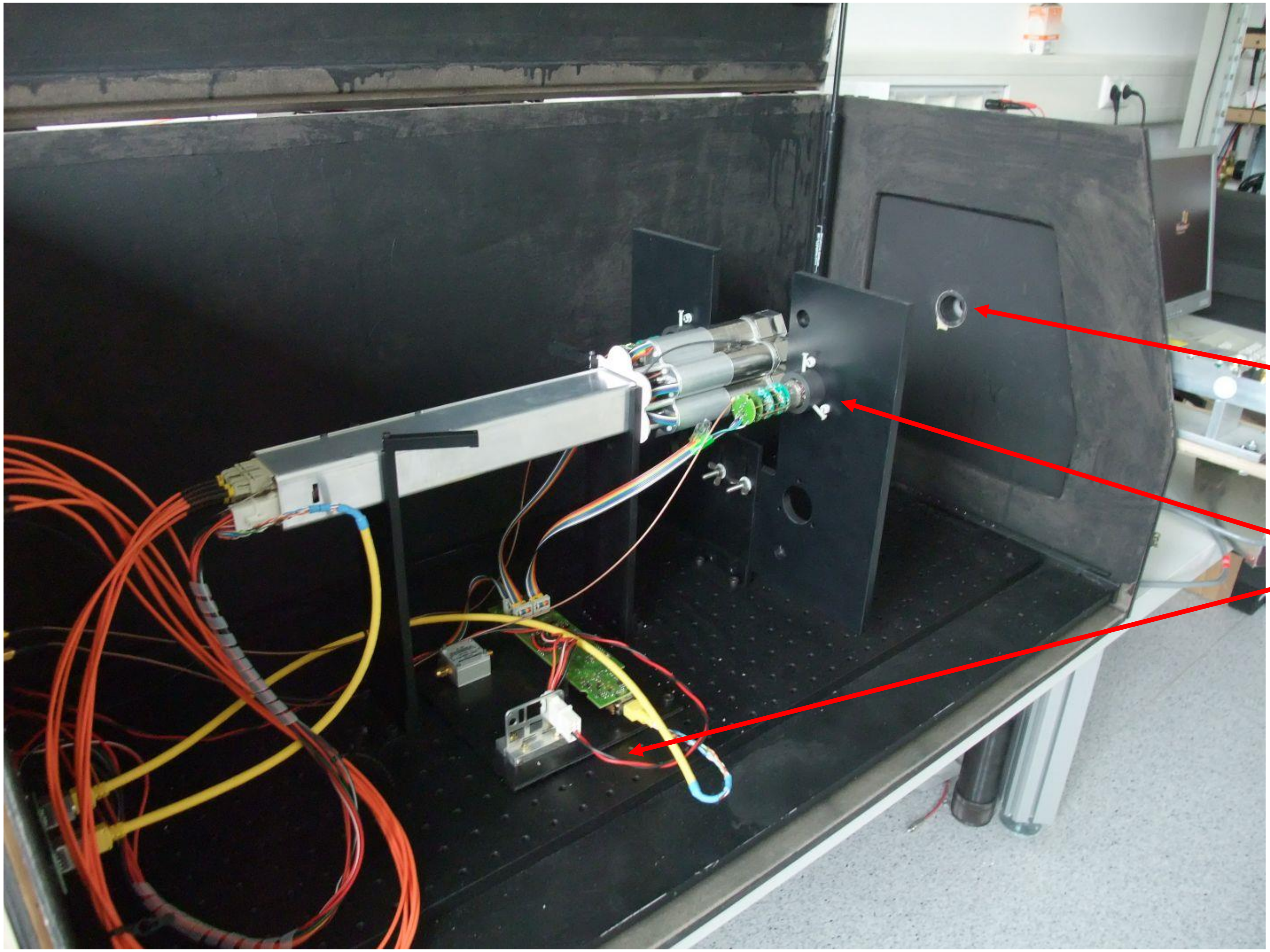

- Side access dark box w/EMI shield (courtesy Toni Engelhardt)
- Ulbricht Sphere exit port
- Monitor PMTs and control

MAGIC Camera Module Measurement -- Setup

- Ulbricht Sphere
- 355 nm laser
- Fixed filter and monitor fiber
- 2x filter wheels
- Similar to camera calibration source

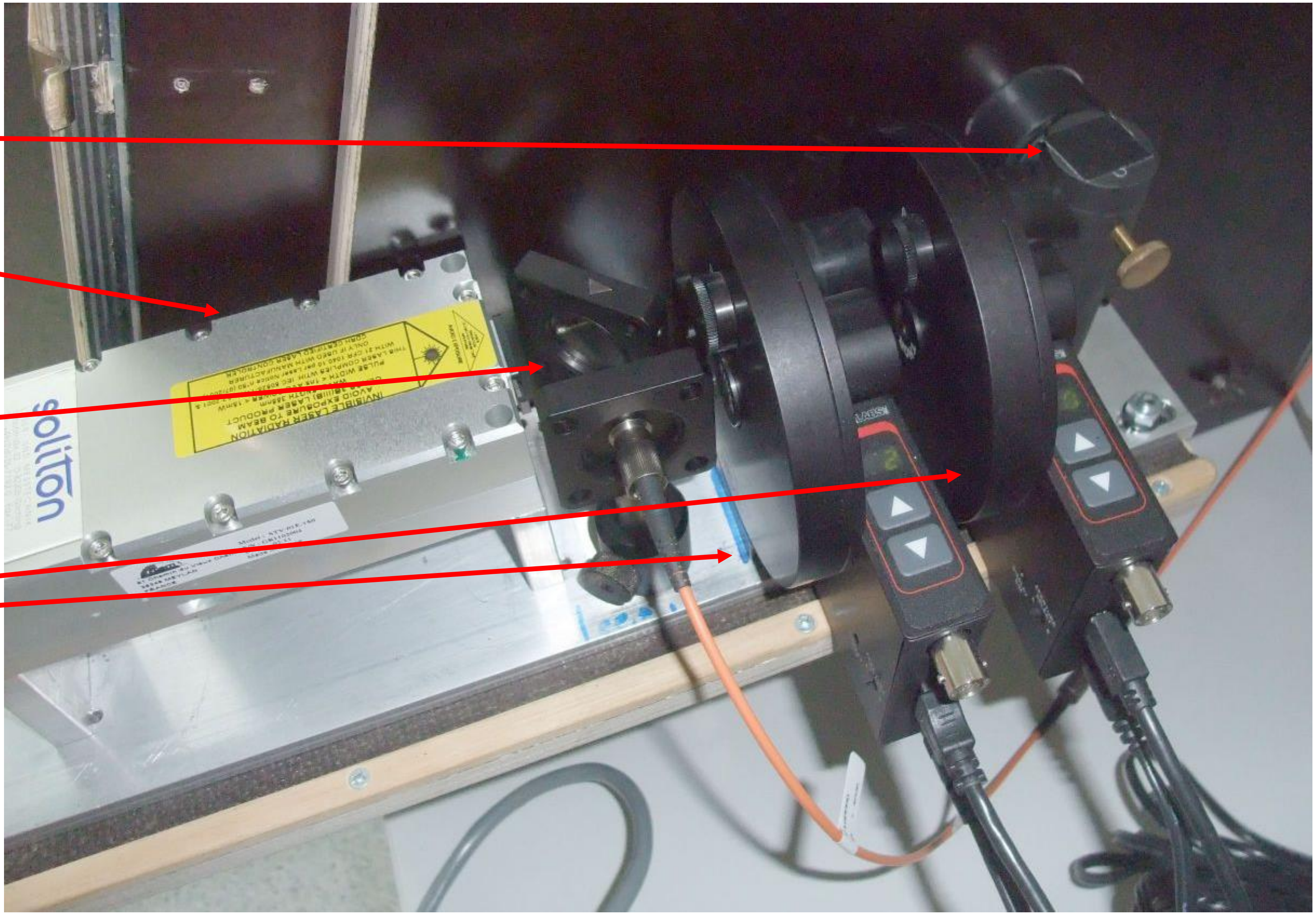

Skipped !

- ID 50
- Croci Gabriele
- Light Response of $LaBr_3$ and YAP Scintillators to 5-20 MeV protons for applications to thin-foil proton recoil neutron spectrometer

Excellent pulse height uniformity response of a new $LaBr_3Ce$ scintillation crystal for gamma ray imaging

R. Pani[1,2], M.N. Cinti[1,2], A. Fabbri[4,5], C. Orlandi[1,2,3], R. Pellegrini[1,5], R. Scafè[1,2]

(1) Department of Molecular Medicine, Sapienza University of Rome, Rome, Italy (2) INFN, Rome 1 Section, Rome, Italy (3) Medical Physics Post Graduate School, Sapienza University of Rome, Rome, Italy (4) Department of Physics, Roma Tre University, Rome, Italy (5)INFN, Rome 3 Section, Rome, Italy

New $LaBr_3Ce$ scintillation crystal

- For small field of view (FOV) detectors based on planar crystals, a reduces pulse height uniformity response is typically obtained in proximity of the crystal edges, due to the absorbent treaatment used for imaging applications, with consequent energy resolution (ER) degradation.
- We propose an analysis on a new $LaBr_3$:Ce scintillation crystal (light yield 63000 photons/MeV, scintillation time 16 ns) with reflective edges that lead up to excellent ER results and pulse height uniformity response, but with dimensions proper for a small FOV gamma imager (50 mm Ø and 6 mm thickness).

New $LaBr_3$:Ce assembly diagram.

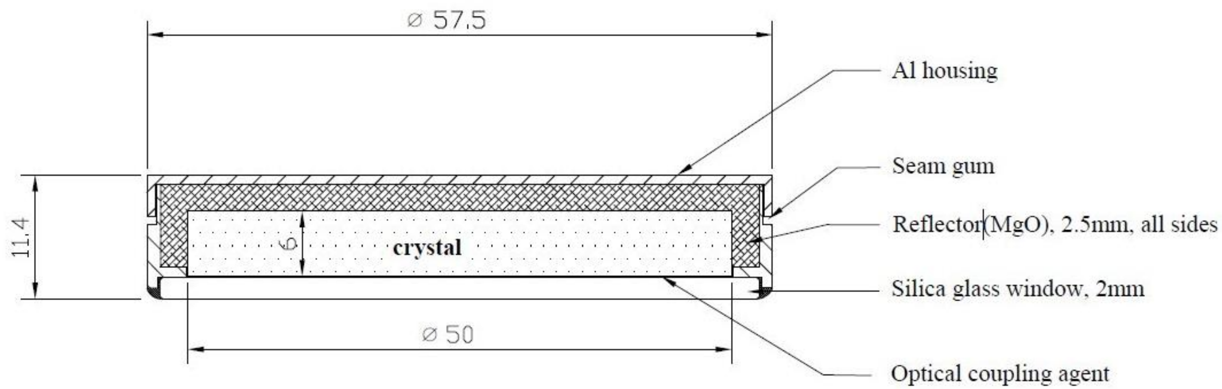

- The performances of the proposed $LaBr_3$:Ce are compared to ones obtained from another $LaBr_3$:Ce with absorbent edge and similar dimensions.
- Both crystals were optically coupled with a Hamamatsu R6231 (PMT) ***(2-inch Ø)*** and a Hamamatsu H10966 ***(52 x 52 mm2)*** MA-PMT used for imaging).
- Two electronic readouts were used: a single channel one for R6231, and a 64 independent channels readout for H10966.

PMTs	Quantum Efficiency (@380nm)	Size (mm)	Gain ($x10^6$)
R6231 PMT	30.0%	51Ø	0.27
H10966 MA-PMT	38.7%	51x51	0.27

ER and pulse height uniformity results

- In the spectrum shown (with R6231), the principal Co^{57} emission peaks (122keV and 136keV) are well discriminated.
- With H10966 MA-PMT local ER results are good on the whole area completely covered by scintillation crystal, without significant ER degradation on the edges. This behavior is due to reflective treatment of surfaces that also leads up to excellent pulse height uniformity response on the whole FOV.

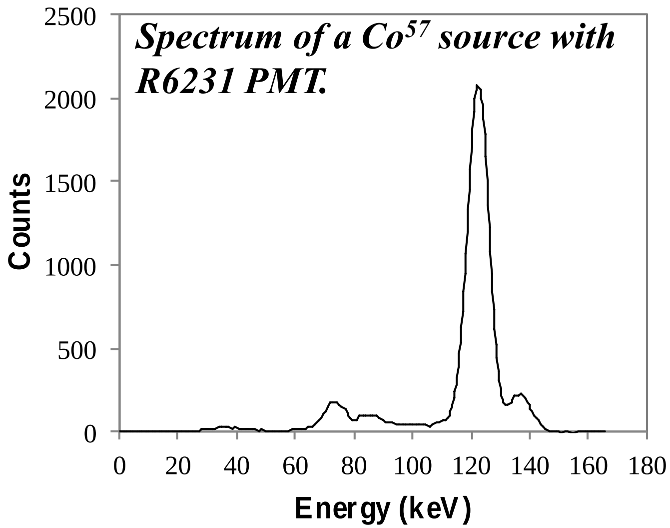

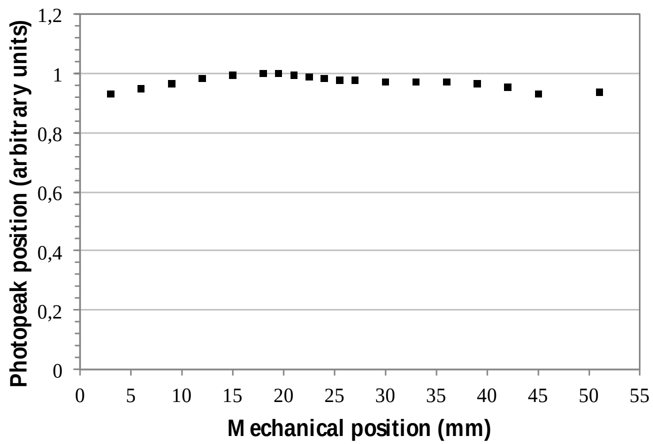

Normalized pulse height uniformity response for the analyzed $LaBr_3$:Ce scintillation crystal optically coupled with Hamamatsu MA-PMT H10966

ENERGY RESOLUTION @122keV (Best Values)		
PMTs	$LaBr_3$:Ce Reflective edges	$LaBr_3$:Ce Absorbent edges
R6231	(6.9±0.3)%	(8.3±0.3)%
H10966	(7.1±0.3)%	(8.4±0.3)%

PULSE HEIGHT UNIFORMITY RESPONSE		
PMTs	$LaBr_3$:Ce Reflective edges	$LaBr_3$:Ce Absorbent edges
R6231	3.0%	24%
H10966	<10%	>10%

Imaging performances

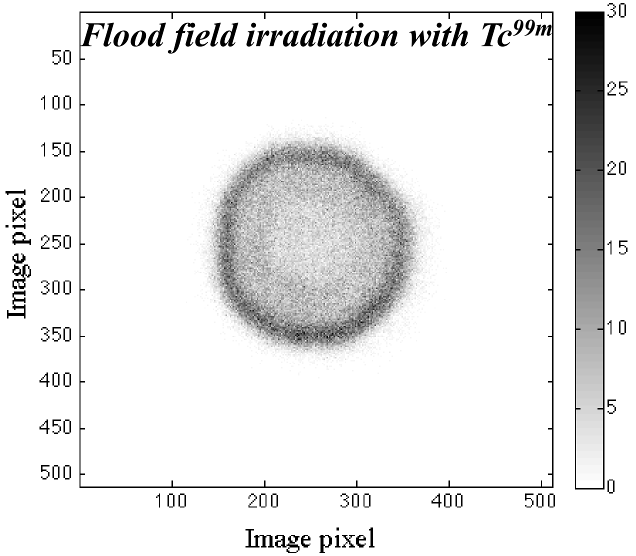

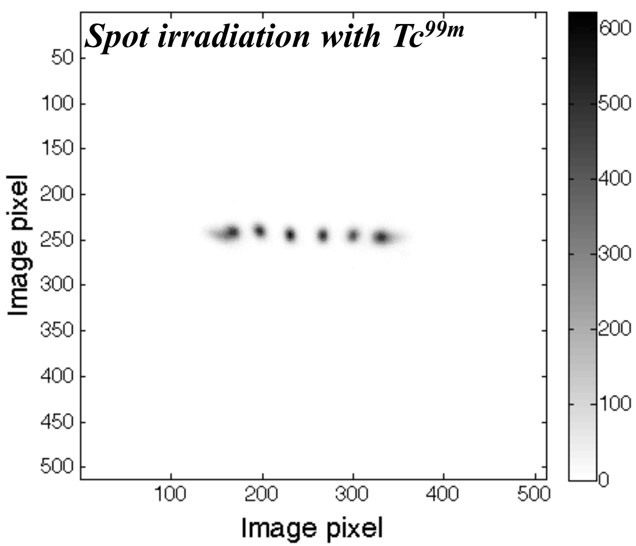

- Traditionally, a crystal with this surfaces treatment is not expected to achieve good imaging performances, due to the compression of the FOV and to a degradation of the linearity.
- Preliminary analysis of scanning data in term of spatial resolution and linearity have shown satisfactory results, when opportune gain correction and position algorithm reconstruction are applied.

INTRINSIC SPATIAL RESOLUTION (mm)	
$LaBr_3$:Ce Reflective edges	$LaBr_3$:Ce Absorbent edges
MEAN VALUE IN CFoV	
1.2	1.0

Skipped !

- ID 56
- Shunsuke Kurosawa
- Perfomance of Ce:La-GPS scintillator with an MPPC

Nanostructured organosilicon luminophores (NOLs) for highly efficient plastic scintillators and spectral sifters

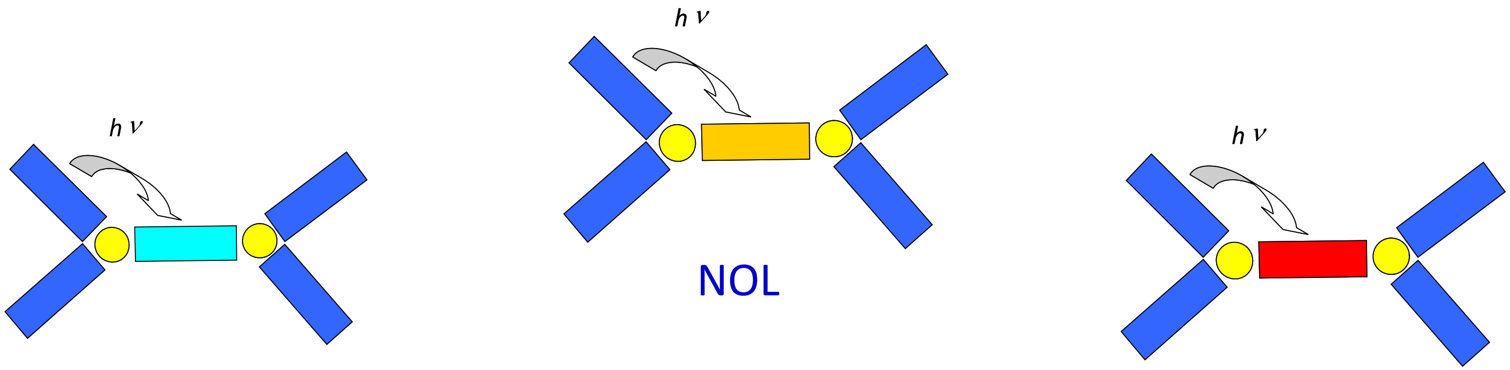

S.A. Ponomarenko[a], N.S. Surin[a], O.V. Borshchev[a], Yu.N. Luponosov[a], E.A. Kleymyuk[a], M.S. Skorotecky[a], D.Y. Akimov[b], A.A. Burenkov[b], A.M. Muzafarov[a]

[a] Enikolopov Institute of Synthetic Polymer Materials, Russian Academy of Sciences, Profsoyuznaya St. 70., 117393 Moscow, Russian Federation.
[b] State Scientific Centre of Russian Federation Institute for Theoretical and Experimental Physics (ITEP), Bolshaya Cheremushkinskaya st. 25, Moscow 117218, Russian Federation.

Classical plastic scintillators and “nanoscintillators”

Classical plastic scintillator

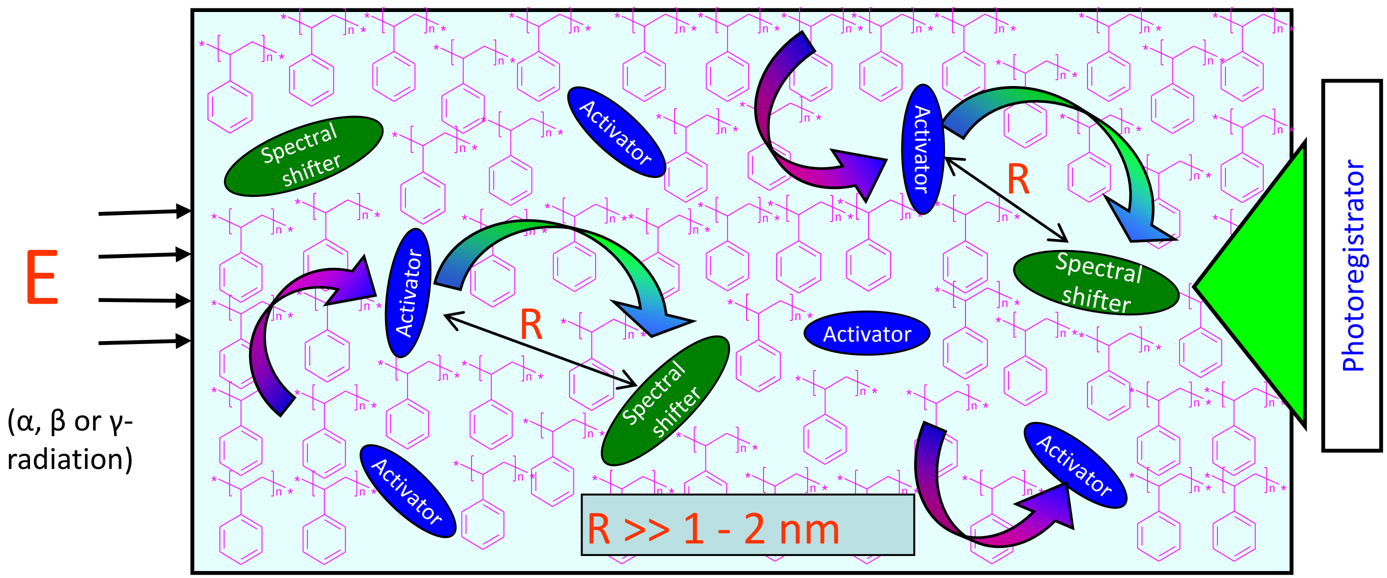

Light output is 45-65% relative to the anthracene standard.

New plastic scintillator with nanostructured organosilicon luminophores (NOLs)

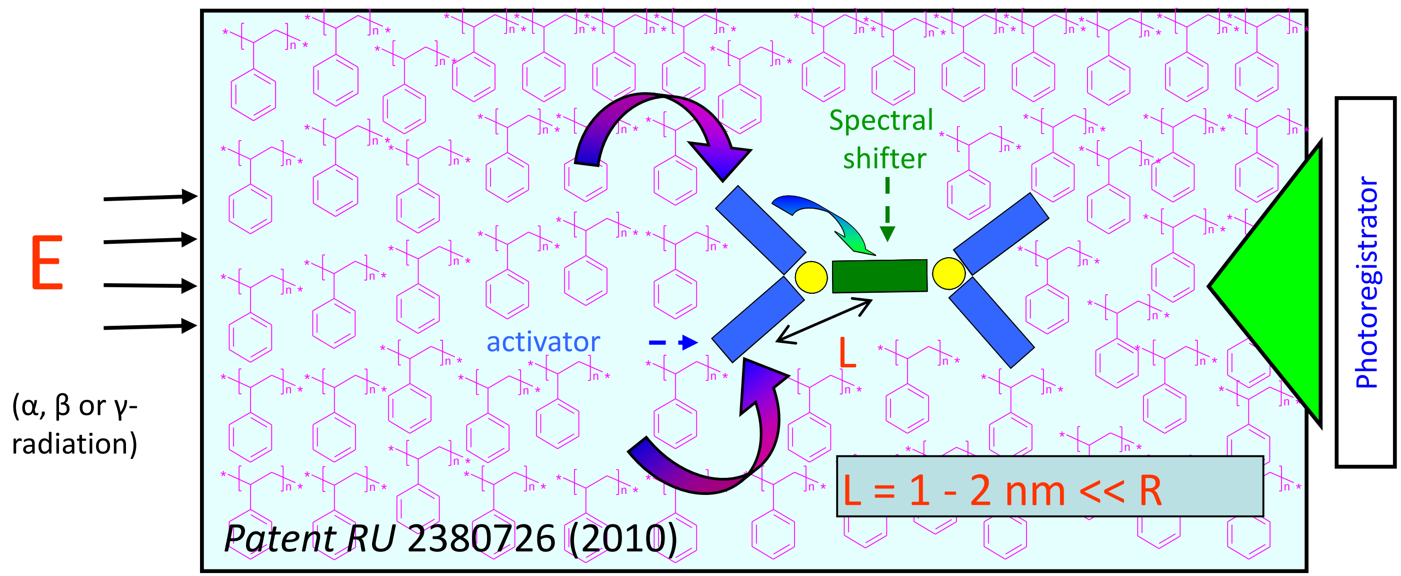

Light output is 90-120% relative to the anthracene standard.

Results of light output and decay time measurements

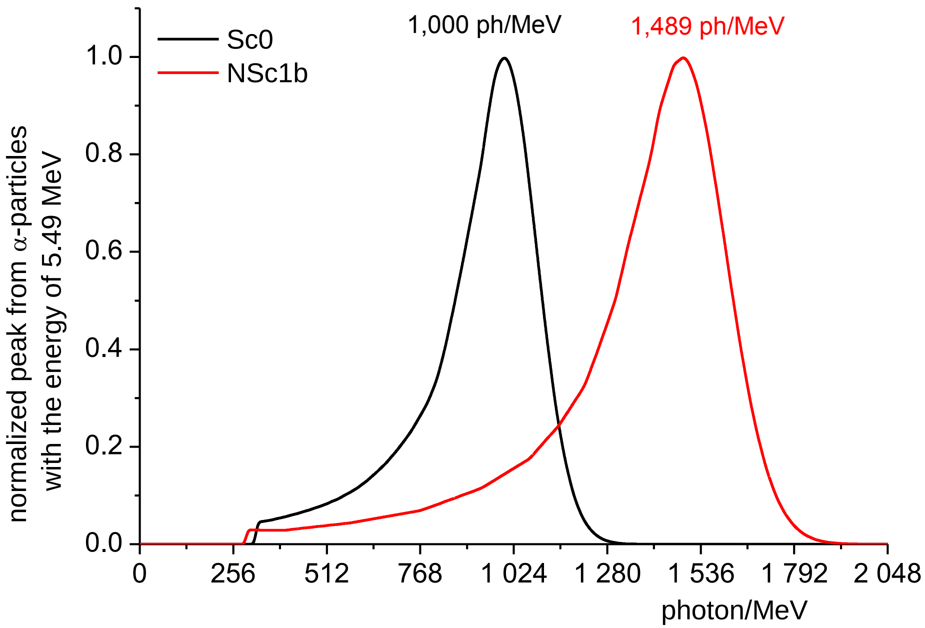

Amplitude spectra, obtained under irradiation of the samples of standard PS scintillator (black) and a new scintillator containing NOLs (red) with α-particles having the energy of 5.49 MeV

Comparison of the scintillation decay times of the standard PS scintillator (blue) and the PS scintillator with NOL (black)

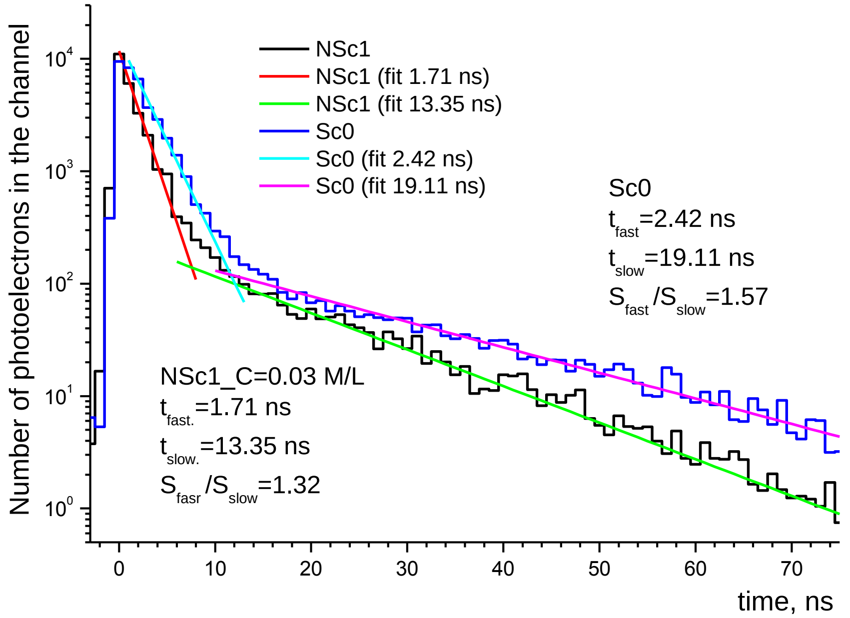

Our approach allows raising the scintillation light output of plastic scintillators on 50% as compared to the standard one, while their scintillation decay time improved on 40%

Plastic scintillators with NOLs having different emission range

Scintillation spectra of a few model polystyrene scintillators - standard Sc0 (black) and with NOLs (colored) having different wavelengths of the emission

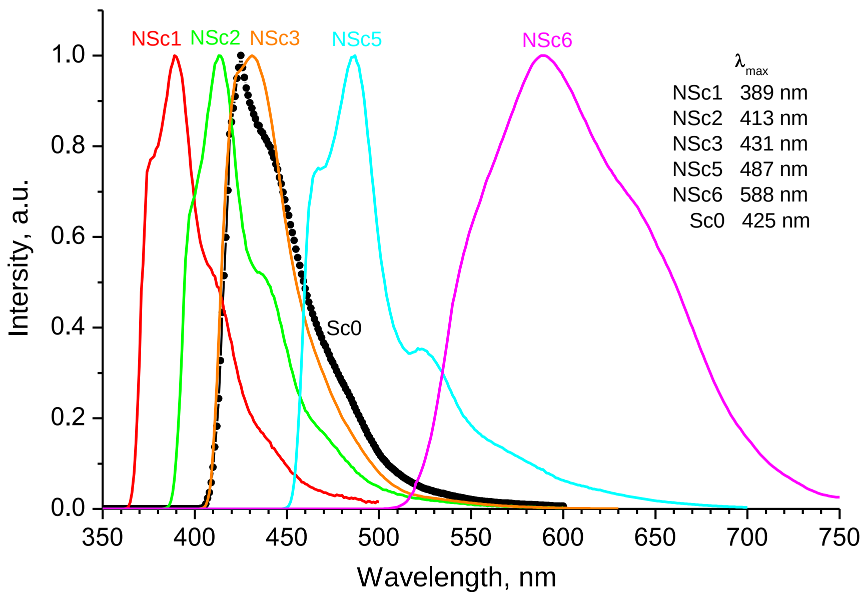

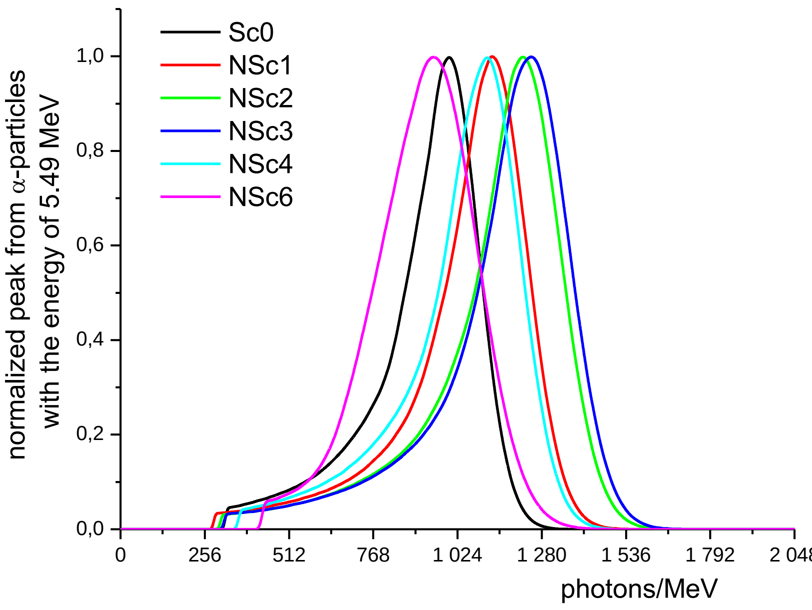

Amplitude spectra, obtained under irradiation of the samples of the standard PS scintillator Sc0 (black) and PS scintillators with NOLs (colored) with the α-particles having the energy of 5.49 MeV

Our approach allows allows tuning the emission of plastic scintillators in a wide spectral region from 390 to 650 nm without loosing their light output, which open possibilities for their application for any type of photodetectors with different spectral sensitivity, as well as for spectral shifters.

Skipped !

- ID 62
- Liu Ben
- FLUKA-based simulation for LYSO gamma detectors in proton therapy

- ID 65
- Kamada Kei
- Development of a proto-type detector using novel Ce:GAGG scintillator arrays for high resolution radiation imaging

"Pilot Production & Commercialization of LAPPD"

LAPPD™ (Large Area Picosecond Photodetector) is a microchannel plate (MCP) based photodetector, capable of imaging, and having both high spatial and temporal resolution in an UHV hermetic package with an active area of 400 square centimeters.

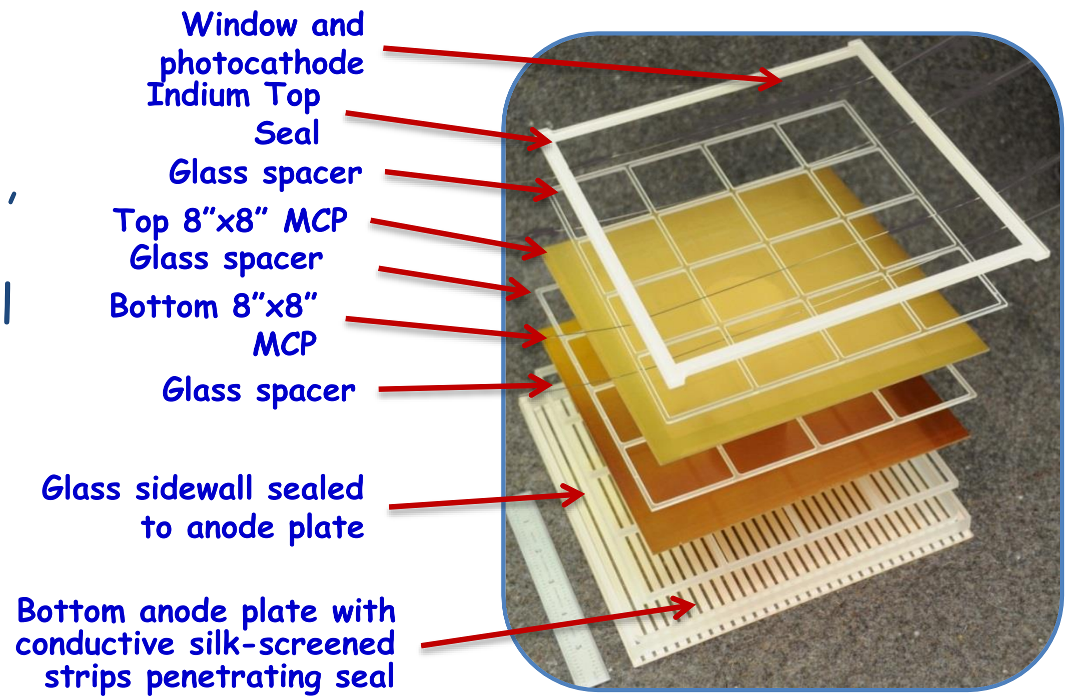

LAPPD™ have a uniquely simple design; a) a hermetic package comprised of top and bottom plates and square sidewall, each made with float glass.

“Next Generation” MCPs

The key breakthrough was the advent of atomic layer deposition (ALD) coating methods and materials to functionalize GCAs converting them into highly effective MCPs with electronic gain and robust performance properties. ALD is characterised by sequential precursor pulsing

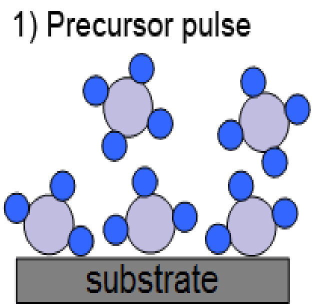

1) Pulse precursor into chamber, which reacts with available sites.

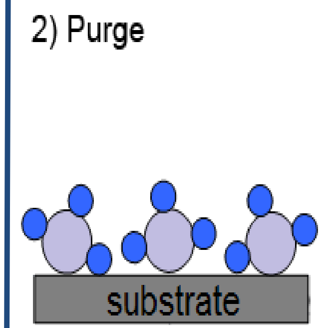

2) Purge to remove by-products. Repeat pulse/purge sequence to grow layers.

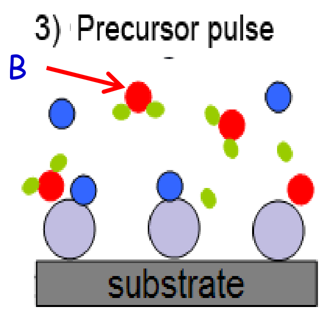

3) Pulse precursor B into chamber, which reacts with available sites. Reaction is self-limiting.

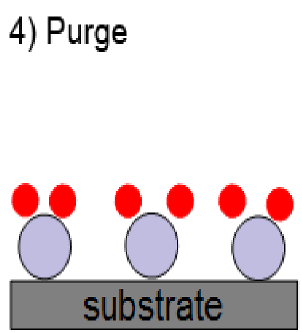

4) Purge to remove unreacted precursors, by-products, and physisorbed species.

Large Area LAPPD with Next Gen MCPs

Advantages of the Incom Next Gen MCPs

- Larger area – 203 mm x 203 mm plates!
- Lead-free – environmentally favorable,
- High aspect ratio with no scrubbing required
- More robust and lower cost

Key Product Feature	Typical	Incom MCP	Incom Advantage
Dark Count	3 cm^{-2} s^{-1}	0.085 cm^{-2} s^{-1}	Enhanced signal to noise
Scrubbing Time	200 h	None required	Lower installed cost
Secondary Electron Yield	3	7	Greater signal amplification
Contains Lead	Yes	No	Environmentally friendly, stronger and more stable
Price (8x8" MCP)	Not Available	Call	Lower cost New applications

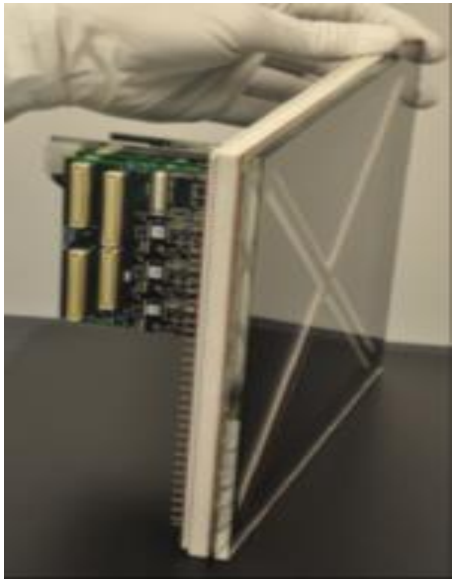

Fully integrated sealed* ceramic LAPPD, with Incom 203mm X 203mm MCP & readout electronics (Gary Varner, U. of Hawaii).

LAPPD Target Specifications

Parameter	Demonstrated Results "Standard" LAPPD 20μ Φ Pores & Future Targets
MCP	Functional area 200 mm x 200 mm x 1.2 mm, 20μ pore Φ, Pitch = 25μ, OAR=65%, Flat ±12.7μ, Resistive Layer: 10-25 megohm, Optional SEE Layer: MgO or Al2O3
MCP Gain	**10^5 @ 1400 Volts, 10^7 @ 2000 Volts,**
MCP Gain Uniformity	**<20%** Edge to edge variability
MCP Background Rates	**3000 sec background, 0.0845 events cm^{-2} sec^{-1}** at 7×10^6 gain, 1025v bias on each MCP. MCP background rate is about 35kHz at the highest running gain.
QE	**20-25% QE** @350-400nm, ±15% uniformity over 200 mmx200 mm area
Spatial Resolution	**1 mm for large signals, 5mm for single photons (application specific)** (With PSEC4 or PSEC5 read-out electronics and software algorithms)
Timing Resolution	**64 ps Demonstrated; Target = ≤40 psec** (610 nm laser, spot image of <5mm, FWHM at high pulse amplitudes)

Optimization of High Count Rate Photon Counting Detector with Microchannel Plates and Quad Timepix readout

A.S. Tremsin, J.V. Vallerga, J.B. McPhate, O.H.W. Siegmund

Space Sciences Laboratory, University of California, Berkeley, California 94720, U.S.A.

Detector configuration and performance

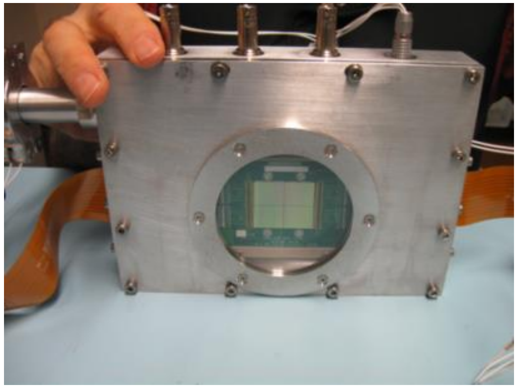

- Detection of photons, ions, neutrons, alphas, high energy electrons, atoms.
- Up to ~25000 simultaneous events can be detected.
- Active area 28x28 mm^2 (2x2 Timepix chips).
- Fast parallel readout (x32) allowing ~1200 frames per second with ~320 μs readout time
- Event centroiding (~15 μm resolution, at ~5×10^6 events/s) or 55 μm resolution at >5×10^8 events/s.
- Time resolution can be ~20 ns at ~2.5×10^7 events/s rates with 55 μm resolution.
- Timing within frames – TOF(energy) or dynamic processes can be studied. Wide energy range or most phases measured in one experiment.

Event centroiding

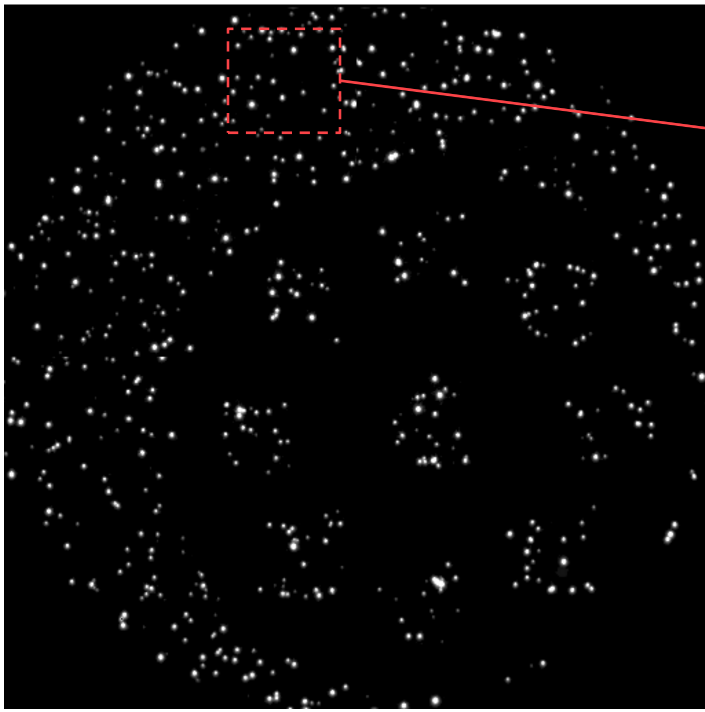

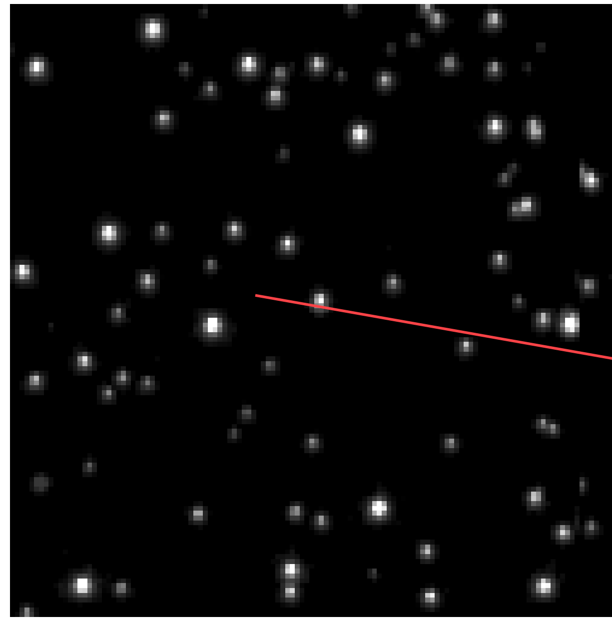

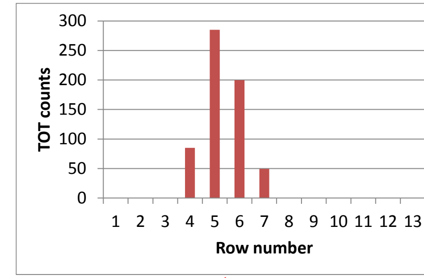

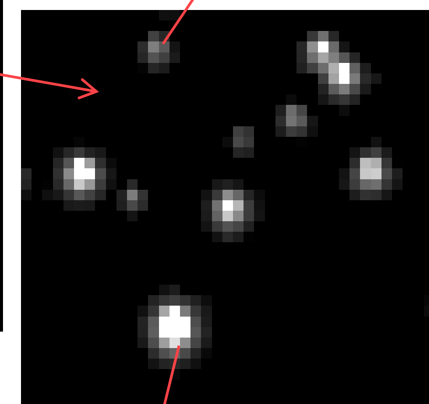

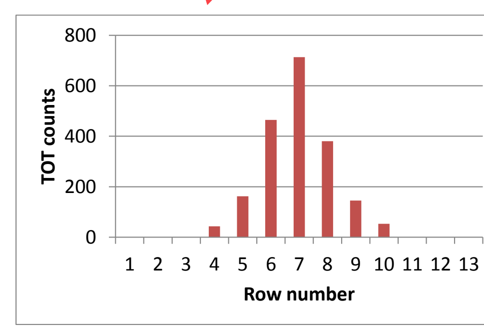

Each pixel measures charge accumulated in a frame (Time Over Threshold method)

Only one event per pixel is allowed in a frame

High resolution imaging through event centroiding

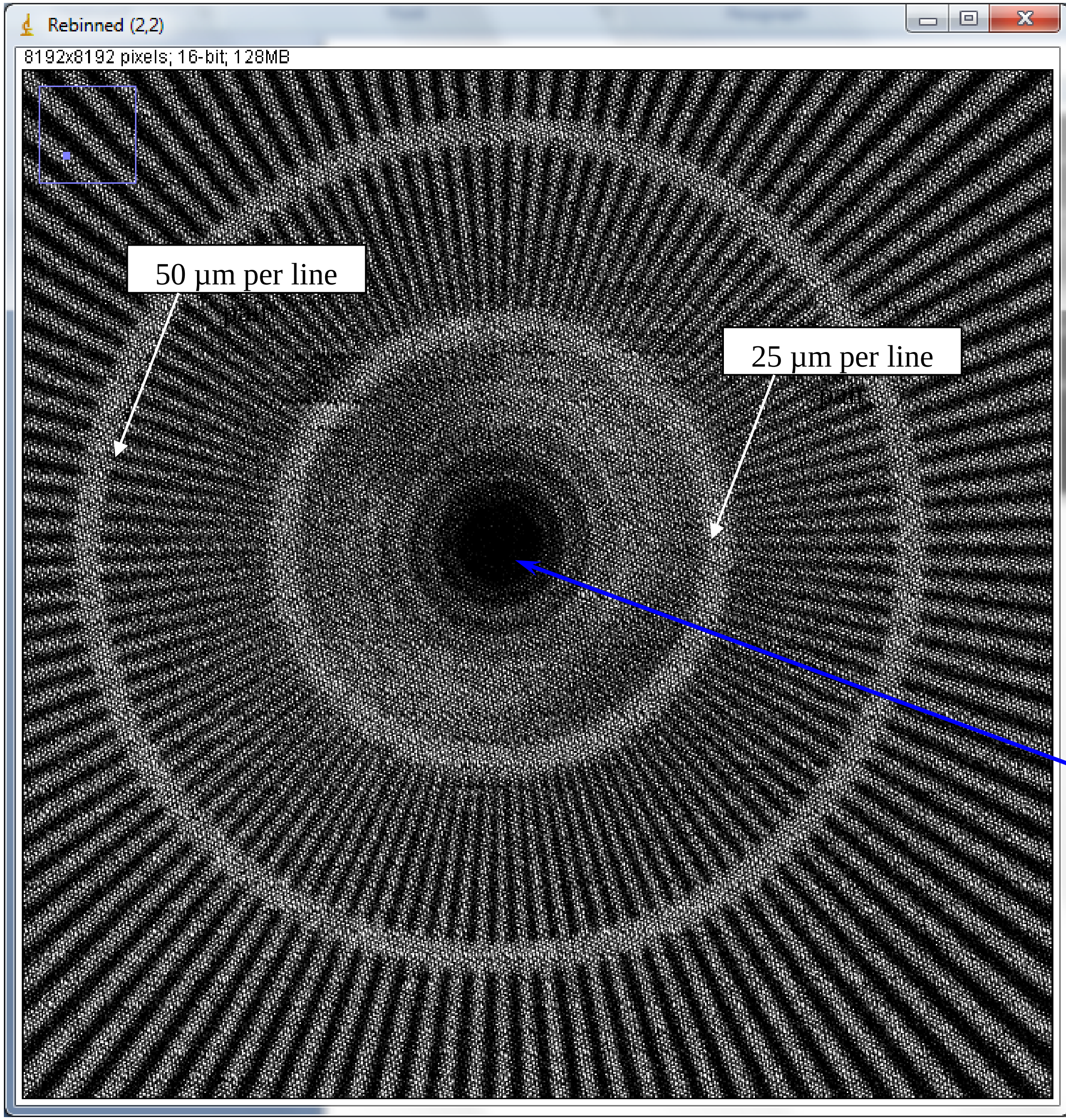

Neutron radiography

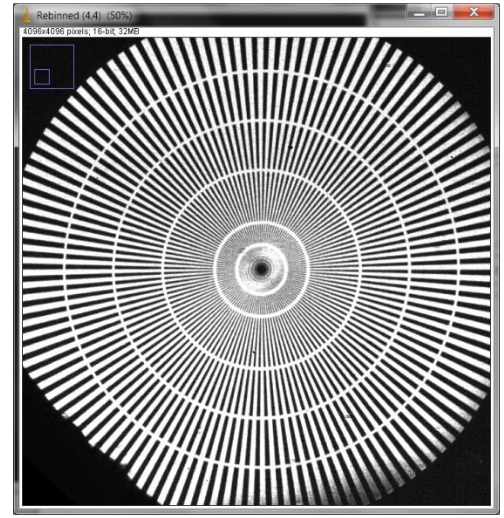

Optical microscope image

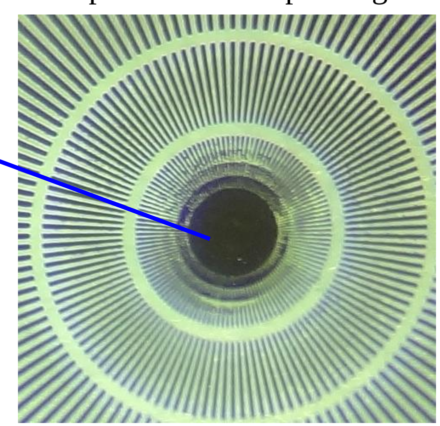

BOA beamline, PSI

UV imaging at high resolution

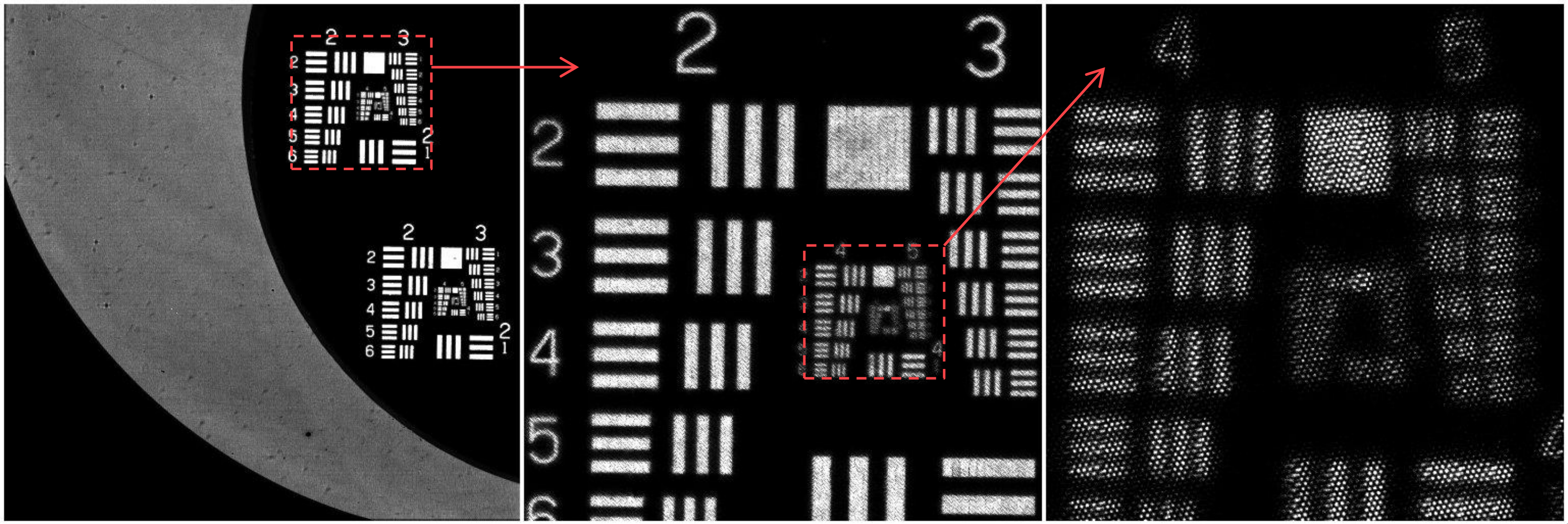

- “Time over threshold” - charge in each pixel instead of counts
- **Charge cloud needs to be optimized for centroiding to sub-pixel accuracy**
- Count rate is limited by frame readout: need to avoid event overlaps

Applications: energy resolved neutron imaging

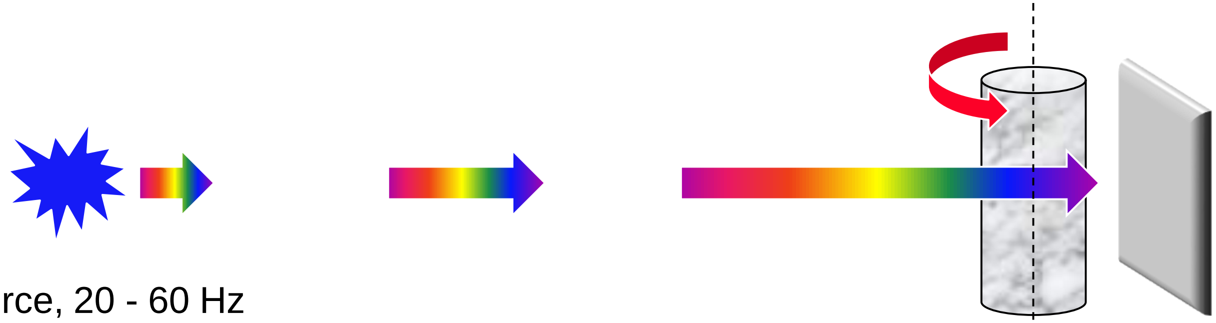

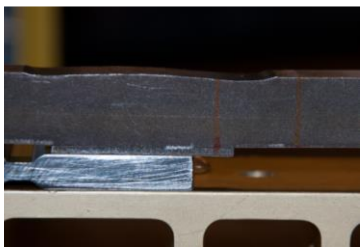

Stir-friction weld

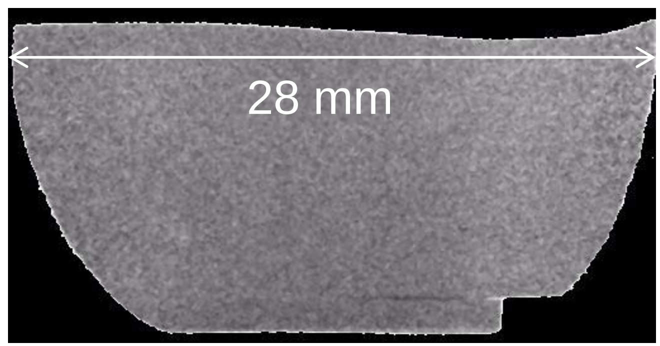

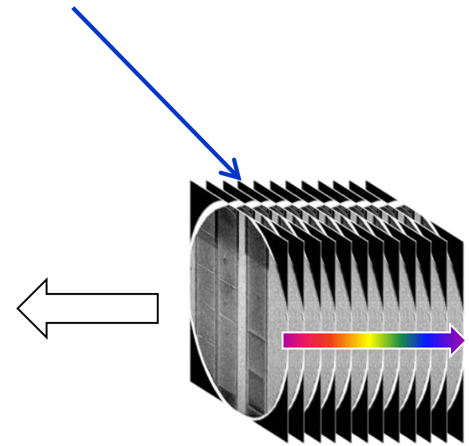

Transmission spectra

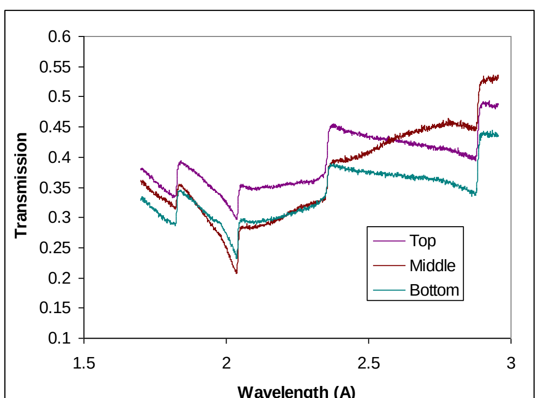

Energy-resolved transmission images.

Measured stack of images, each corresponds to ΔE

Strain mapping in Ni bolt

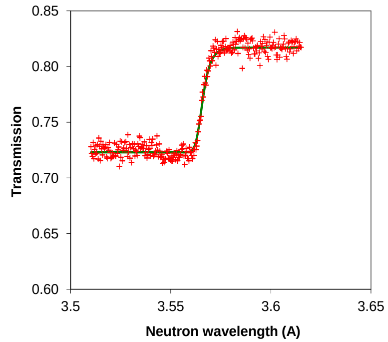

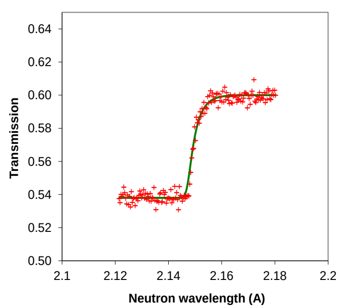

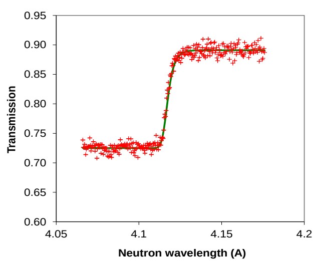

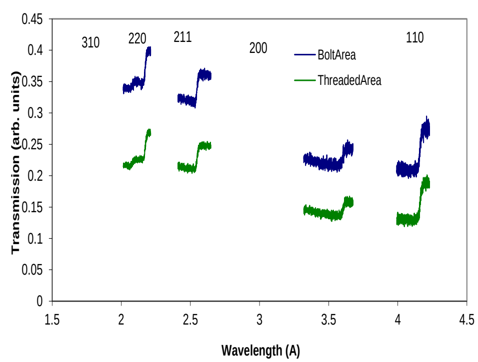

Strain 4.16A edge

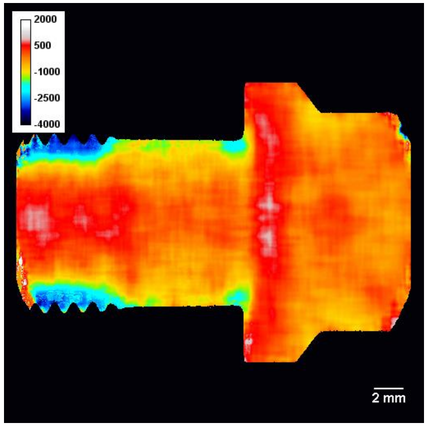

Edge height

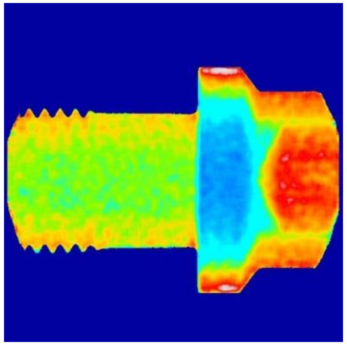

Strain 2.14A edge

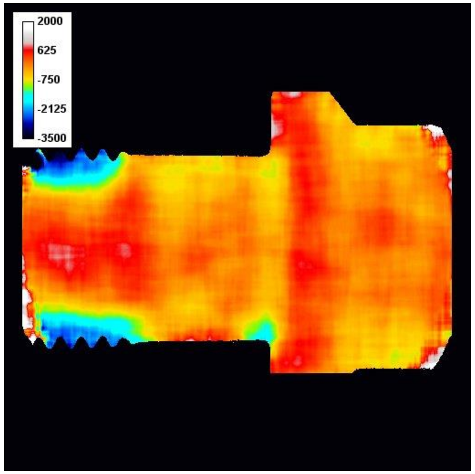

Edge Pedestal

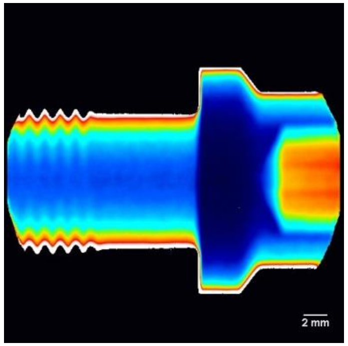

Resonance transmission spectra

1.18 mm Ta foil: measured and theoretical transmission

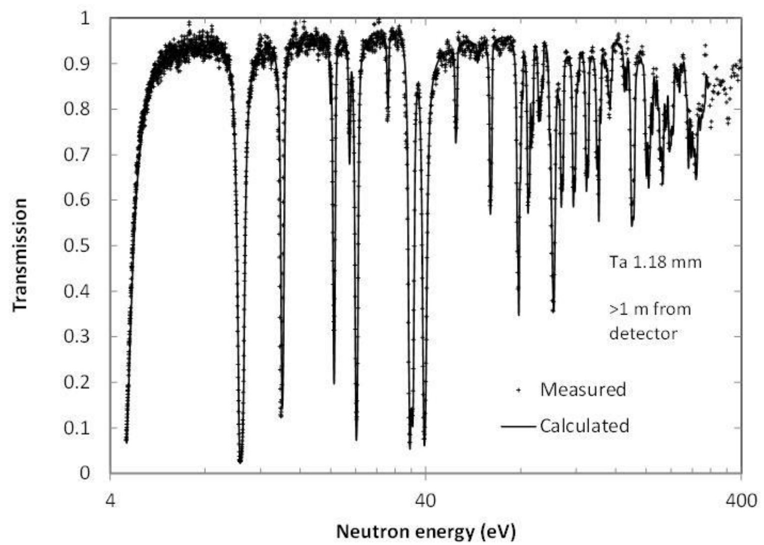

Ag of various thickness